The organization of the human cerebellum estimated by intrinsic functional connectivity

Randy L. Buckner, Fenna M. Krienen, Angela Castellanos, Julio C. Diaz and B. T. Thomas Yeo

J Neurophysiol 106:2322-2345, 2011. First published 27 July 2011;
doi: 10.1152/jn.00339.2011

J Neurophysiol 106: 2322–2345, 2011.
First published July 27, 2011; doi:10.1152/jn.00339.2011.

The organization of the human cerebellum estimated by intrinsic functional connectivity

Randy L. Buckner,[1,2,3,4] Fenna M. Krienen,[2,4] Angela Castellanos,[1,2] Julio C. Diaz,[1,5] and B. T. Thomas Yeo[2,4]

[1]*Howard Hughes Medical Institute, Cambridge;* [2]*Center for Brain Science, Department of Psychology, Harvard University, Cambridge;* [3]*Department of Psychiatry, Massachusetts General Hospital, Boston;* [4]*Athinoula A. Martinos Center for Biomedical Imaging, Department of Radiology, Massachusetts General Hospital, Charlestown, Massachusetts; and* [5]*Department of Biology, University of Miami, Miami, Florida*

Submitted 13 April 2011; accepted in final form 20 July 2011

Buckner RL, Krienen FM, Castellanos A, Diaz JC, Yeo BT. The organization of the human cerebellum estimated by intrinsic functional connectivity. *J Neurophysiol* 106: 2322–2345, 2011. First published July 27, 2011; doi:10.1152/jn.00339.2011.—The cerebral cortex communicates with the cerebellum via polysynaptic circuits. Separate regions of the cerebellum are connected to distinct cerebral areas, forming a complex topography. In this study we explored the organization of cerebrocerebellar circuits in the human using resting-state functional connectivity MRI (fcMRI). Data from 1,000 subjects were registered using nonlinear deformation of the cerebellum in combination with surface-based alignment of the cerebral cortex. The foot, hand, and tongue representations were localized in subjects performing movements. fcMRI maps derived from seed regions placed in different parts of the motor body representation yielded the expected inverted map of somatomotor topography in the anterior lobe and the upright map in the posterior lobe. Next, we mapped the complete topography of the cerebellum by estimating the principal cerebral target for each point in the cerebellum in a discovery sample of 500 subjects and replicated the topography in 500 independent subjects. The majority of the human cerebellum maps to association areas. Quantitative analysis of 17 distinct cerebral networks revealed that the extent of the cerebellum dedicated to each network is proportional to the network's extent in the cerebrum with a few exceptions, including primary visual cortex, which is not represented in the cerebellum. Like somatomotor representations, cerebellar regions linked to association cortex have separate anterior and posterior representations that are oriented as mirror images of one another. The orderly topography of the representations suggests that the cerebellum possesses at least two large, homotopic maps of the full cerebrum and possibly a smaller third map.

somatotopy; motor control; prefrontal; functional magnetic resonance imaging; default network; connectome

THE ORGANIZATION OF THE CEREBELLUM has been the topic of debate for more than a century (Manni and Petrosini 2004). Although there is agreement that the cerebellum contains multiple somatomotor representations, a challenging feature of cerebellar anatomy prevents resolving its complete organization: the cerebellum is connected to the cerebral cortex only by way of polysynaptic circuits (Evarts and Thach 1969; Kemp and Powell 1971; Schmahmann and Pandya 1997a; Strick 1985). Efferent projections from the cerebrum synapse initially in the pontine nuclei and then project primarily to the contralateral cerebellar cortex (the pontocerebellar tract). Afferent projections first synapse in the deep cerebellar nuclei (e.g., dentate nucleus) and then project to a second synapse in the contralateral thalamus that in turn serves as a relay to the cerebral cortex (the dentatothalamocortical tract). There are no monosynaptic connections between the cerebrum and cerebellum. As a result, traditional anterograde and retrograde tracing techniques cannot be used to explore the relation between cerebral topography and the cerebellum. Insights into cerebellar organization require physiological and transneuronal tracing techniques, inferences from deficits following lesions, and functional neuroimaging studies.

Somatomotor Topography in the Cerebellum

Early electrophysiological studies revealed that the cerebellum possesses multiple topographically organized somatomotor[1] representations (Adrian 1943; Snider and Sowell 1944). An inverted somatomotor map is present in the anterior lobe, and a second posterior map is upright, forming an inversion between the anterior and posterior representations. Evidence directly demonstrating that cerebral motor areas are anatomically connected to specific regions of the cerebellum came with the development of transneuronal tracing techniques. Transneuronal tracing techniques use virus strains that selectively spread through retrograde or anterograde infection of synaptically connected neurons (HSV1; Middleton and Strick 1994, 2001; rabies virus; Kelly and Strick 2003). With the use of viral tracing, the hand region of cebus monkey cerebral M1 was found to possess both efferent and afferent polysynaptic projections to lobules V and VI (the anterior lobe somatomotor representation) and HVIIB/HVIII in the posterior lobe (Kelly and Strick 2003). The intervening posterior lobules, in particular Crus I and II, were spared anatomical connections to motor cortex but did show projections to prefrontal cortex, an important observation that is discussed in more detail below.

Human neuroimaging studies have confirmed somatomotor representations within the cerebellum. In a particularly thorough exploration using task-based functional MRI (fMRI), Grodd et al. (2001) had subjects make movements that revealed maps of both gross motor topography (foot, hand, tongue, and lips) as well as fine motor topography (elbow,

Address for reprint requests and other correspondence: R. L. Buckner, Harvard Univ., 52 Oxford St., Northwest Bldg., 280.06, Cambridge, MA 02138 (e-mail: randy_buckner@harvard.edu).

[1] Here and elsewhere the term "somatomotor" is chosen because it is difficult to resolve whether cerebellar representations of body space are selectively linked to motor cortex or somatosensory cortex.

wrist, and multiple individuated finger movements). An inverted representation was detected extending from lobule V of the anterior lobe (foot, arm, and fingers) to just past the primary fissure in lobule VI (tongue and lip representation). A second upright representation was detected in VIII and IX. Wiestler et al. (2011) recently used high-resolution fMRI data acquisition to localize the representation of the fingers to lobules V and VIII. Relevant to the present article, the well-characterized somatomotor representations provide a target for validating new human neuroimaging techniques.

Uncharted Regions of the Cerebellum

In the monkey, the anterior somatomotor representation extends just past the primary fissure with the face localized to the simplex lobule (HVI) (Snider and Eldred 1952). The second posterior representation is near the paramedian lobule (HVIII). The relation between the two representations is that of inversion, much like the mirror-image representations of the visual field that exist between certain visual areas (e.g., V1 and V2; Cowey 1964). However, unlike maps of retinal space within early visual cortex, which are contiguous with one another (Van Essen et al. 1982; Wandell et al. 2007), the identified somatomotor maps of the cerebellum leave a large gap between the two detected representations. This raises an important question that we attempt to address in this article: What is mapped to the intervening regions of the cerebellum?

One possibility is that multiple repeated somatomotor maps exist, creating a set of regions within the cerebellum that have different or elaborated representations of motor space. Consistent with the possibility that the uncharted regions of the cerebellum contain multiple somatomotor maps, Schlerf et al. (2010) recently found preliminary evidence for a second somatomotor map posterior to the primary fissure. In their study, complex finger and toe movements (involving sequences of extension and flexion across digits) showed more extensive activation than simple movements with the toe response extending posterior to the finger response, raising the possibility of a second adjacent representation. The novel map is hypothesized to participate when complex skilled movements are performed but less so when simple movements are initiated. Somatomotor maps with novel properties may occupy a portion of the remaining cerebellar cortex.

A second possibility is that the cerebellum is mapped to cerebral regions outside the domain of motor function, including areas implicated in cognition. Although we provide evidence in this article to support this second possibility, it is important to note past findings that have caused opposition to this idea. Foremost, cerebellar lesions result in profound motor deficits; cognitive deficits exist but are more subtle (Ben-Yehudah et al. 2007; Schmahmann et al. 2007; Timmann and Daum 2007). Early physiological and anatomical studies did search for cerebellar connections with prefrontal association cortex but found only selective examples (Brodal 1978; Glickstein et al. 1985; Snider and Eldred 1952). As a result of these anatomical findings, many theories addressing the cerebellum's evolutionary expansion emphasized motor skills, including volitional control of hand movements (e.g., Glickstein 2007; Holmes 1939). However, a seminal theoretical report by Leiner et al. (1986; see also Leiner 2010) and a series of unexpected findings from the emerging field of human neuroimaging (Petersen et al. 1989) rekindled interest in the idea that the cerebellum may interact with the prefrontal cortex and be important to cognition.

Activation of the cerebellum during cognitive tasks has been a common observation (Desmond and Fiez 1998; Timmann and Daum 1997), leading to several explorations of the functional meaning of the responses (e.g., Durisko and Fiez 2010; Marvell and Desmond 2010; O'Reilly et al. 2008; Spencer et al. 2007). Recently, Stoodley and Schmahmann (2009) conducted a meta-analysis of previously published articles that reported cerebellar activations across a range of sensory, motor, and cognitive tasks. By using a meta-analytic approach that generates spatial maps of consensus responses (Laird et al. 2005), they observed several features of human cerebellar organization. First, different task domains elicit activation in distinct cerebellar regions. As expected, anterior and posterior regions near to or containing the body representations emerge from tasks that have motor demands. Second, the expanse of the cerebellum occupied by Crus I and lobules VI and VII shows consensus activation during tasks that place demands on cognitive functions including language, working memory, and executive function. These results reinforce the possibility that regions of the cerebellum between the known somatomotor representations contribute to higher level cognition. The expansion of these regions in the human cerebellum may parallel the expansion of association cortex, including prefrontal cortex (e.g., see Balsters et al. 2010 for a recent discussion).

Anatomical Evidence for Prefrontal-Cerebellar Circuits

Using anterograde tracing techniques, Schmahmann and Pandya (1997b) identified projections from dorsolateral and rostral regions of prefrontal cortex including areas 9, 46, and 10 to the pontine nuclei. The presence of pontine-labeled neurons indicates that a cerebrocerebellar projection exists, albeit without specifying where the projection terminates within the cerebellar cortex. Transneuronal tracing techniques have revealed both efferent and afferent cerebellar projections to the prefrontal cortex (Kelly and Strick 2003; Middleton and Strick 1994, 2001; see Strick et al. 2009 for review). Middleton and Strick (1994, 2001) first used transneuronal retrograde tracing to show that prefrontal areas 9m, 9l, and 46 receive polysynaptic projections from the dentate nucleus. Later advances allowed direct visualization of both anterograde transport (using HSV1) and retrograde transport (using rabies virus) between prefrontal cortex and the cerebellar cortex itself (Kelly and Strick 2003). Area 46 was found to possess polysynaptic projections to cerebellar regions that were spared motor projections. Prefrontal efferents labeled with HSV were found in Crus II extending into Crus I but were absent in the anterior lobe. Prefrontal afferents labeled with rabies virus were found in Crus II.

The findings of Strick and colleagues are important to the present work for two reasons. First, the results suggest that a significant portion of the cerebellum between the anterior and posterior somatomotor representations is linked to cerebral association cortex. Given that association cortex is disproportionately expanded in humans relative to monkeys and even apes (Hill et al. 2010; Preuss 2004; Van Essen and Dierker 2007), it is possible that a majority of the cerebellum is connected to association cortex in the human. Second, the

results reveal that multiple closed-loop cerebellar circuits exist in parallel. The region of the cerebellum that receives projections from area 46 sends projections back to prefrontal area 46; this region is anatomically distinct from the cerebellar regions receiving and sending projections to somatomotor cortex. The presence of multiple, segregated cerebrocerebellar circuits provides an opportunity to map cerebellar topography using human neuroimaging techniques by examining functional coupling between the two structures.

Functional Connectivity Provides a Tool to Map Cerebellar Organization

Intrinsic low-frequency functional correlations measured by fMRI can be used to map brain systems in the human (see Fox and Raichle 2007; Raichle 2011; Van Dijk et al. 2010 for review). Biswal et al. (1995) first described the approach. They observed that activity fluctuations within the motor cortex measured at rest demonstrate functional coupling with the contralateral motor region and the supplementary motor region along the medial wall. The correlations were anatomically selective, suggesting the tool could be used for mapping. Since then, numerous studies have used this approach, termed functional connectivity MRI (fcMRI), to map brain systems including subdivisions of the cingulate (Margulies et al. 2007), hippocampal formation (Kahn et al. 2008), amygdala (Roy et al. 2009), thalamus (Zhang et al. 2008), and striatum (Di Martino et al. 2008). fcMRI has limitations and interpretational difficulties, including sensitivity to factors other than anatomical connectivity (Buckner 2010; Cole et al. 2010; Moeller et al. 2009). We discuss these limitations later when interpreting results of the present study. Relevant first is that, even with these limitations, fcMRI is a potentially powerful technique for mapping cerebrocerebellar circuits.

Initial fcMRI studies of the cerebellum reported multiple results that are consistent with known anatomical properties of cerebrocerebellar circuits (Allen et al. 2005; Habas et al. 2009; Krienen and Buckner 2009; O'Reilly et al. 2010). First, intrinsic activity measured from lateralized seed regions in the frontal motor cortex is correlated with the contralateral cerebellum more so than the ipsilateral cerebellum. This functional observation is consistent with the anatomical finding that the majority of cerebrocerebellar projections are contralateral. Second, the functionally coupled motor regions fall within the anterior and posterior lobe locations predicted by task-based analysis of human somatomotor topography. This result indicates that the technique is anatomically specific as well as sensitive, because both the primary (anterior lobe) and secondary (posterior lobe) somatomotor representations can be detected (e.g., Fig. 1 of Krienen and Buckner 2009; Fig. 1 of O'Reilly et al. 2010). Third, lateralized infarcts to the basilar pons selectively disrupt contralateral but not ipsilateral functional coupling between the cerebrum and cerebellum (Lu et al. in press) as predicted by anatomical studies (Schmahmann et al. 2004a, 2004b).

Prior fcMRI studies also have observed that a major portion of the human cerebellum is functionally coupled to cerebral association areas (Habas et al. 2009; Krienen and Buckner 2009; O'Reilly et al. 2010). These studies generally agree about the topography of association regions of the cerebellum despite the use of different analytic approaches and data samples. For example, they all reported nearly the same locations for human cerebellar somatomotor cortex and also observed that Crus I and II were coupled to cerebral association areas falling within dorsolateral prefrontal cortex and parietal association cortex.

The most marked difference between studies occurred in relation to the estimates of the cerebellar zones coupled to the human "default network" (Buckner et al. 2008; Raichle et al. 2001; see Yeo et al. 2011 for relevant discussion). Although both Habas et al. (2009) and Krienen and Buckner (2009) noted that a cerebellar region associated with the default network exists within lobule IX, Krienen and Buckner reported a second major region in Crus I. This difference led the two reports to emphasize distinct cerebellar regions associated with the default network: one report focused on lobule IX and the other on Crus I. This difference may arise from an omission rather than a true discrepancy. Habas et al. (2009) did not assign the portion of Crus I in question to any identifiable cerebral network; rather, there is an absence of a network assignment in the exact region proposed to align with the default network in Krienen and Buckner (2009). Thus a careful assessment of the prior reports suggests general agreement, with the few differences possibly arising because each study did not comprehensively survey the cerebellum. These initial results encourage further exploration.

In this study we mapped the complete topography of the human cerebellum. In doing so, we sought to extend prior work to determine whether there were any mapping principles between the cerebral cortex and the cerebellum. By mapping the full extent of the cerebellum to the cerebral cortex, we were able to examine whether there were any expansions and restrictions in the representations of specific cortical networks in the cerebellum and, as a consequence, examine the orderly representation of different functional domains in the cerebellum. We discovered that the cerebellum possesses multiple representations of the cerebrum in which the known somatomotor representations are parts of at least two, and possibly three, homotopic maps of the full cerebrum.

METHODS

Overview

In the present study, we explored the functional organization of the human cerebellum using resting-state fcMRI. Analyses proceeded in three phases. First, cerebrocerebellar circuitry of the somatomotor cortex was explored because of the strong expectations about the location and topographic organization of the body representations. Data were acquired from 26 subjects while they performed active movements of the foot, hand, or tongue. Motor task activation was used to estimate somatomotor topography. The somatomotor topography of the cerebellum was then analyzed in 1,000 young adults by exclusively using functional connectivity of resting-state data. The motor task data served as the reference.

Second, having established that basic properties of cerebellar topography can be revealed by intrinsic functional connectivity, we next mapped the full extent of the cerebellar cortex. The cerebral networks defined in the companion paper by Yeo et al. (2011) provided the basis for this analysis. The strategy was to ask, for each voxel within the cerebellum, to which cerebral network it was most strongly correlated. This approach yielded a complete map of the cerebellum that represented regions of the cerebellum coupled to distinct regions of the cerebrum.

The final analyses sought to quantify in more detail functional connectivity between the cerebellum and cerebrum. The strategy was to define small seed regions within the cerebellum and map the functionally correlated topography in the cerebral cortex, and to estimate functional correlation strength between cerebellar regions and multiple cerebral regions to quantify specificity. These analyses did not assume that the a priori cortical networks used for the above analyses were correct. For these analyses, cerebral and cerebellar regions were always defined in the discovery sample ($n = 500$) and functional connectivity was only quantified in the independent replication sample ($n = 500$) to avoid bias.

Participants

Paid participants were clinically normal, English-speaking young adults with normal or corrected-to-normal vision (ages 18–35 yr). Subjects were excluded if their fMRI signal-to-noise ratio (SNR) was low (<100; see Yeo et al. 2011), artifacts were detected in the MR data, their self-reported health information indicated a history of neurological or psychiatric illness, or they were taking psychoactive medications. Two data sets were used for analysis. The first data set involved task-based data collected while subjects made active motor movements ($n = 26$, mean age = 21.3 yr, 50% male). The data set for functional connectivity analysis consisted of 1,000 individuals imaged during eyes open rest (EOR) and was divided into two independent samples (each $n = 500$; labeled the discovery and replication samples). Age and sex were matched for the discovery (mean age = 21.3 yr, 42.6% male) and replication (mean age = 21.3 yr, 42.8% male) samples as described in Yeo et al. (2011). Participants provided written informed consent in accordance with guidelines set by institutional review boards of Harvard University or Partners Healthcare.

MRI Data Acquisition

All data were collected on matched 3T Tim Trio scanners (Siemens, Erlangen, Germany) using the vendor-supplied 12-channel phased-array head coil. The functional imaging data were acquired using a gradient-echo echo-planar imaging (EPI) sequence sensitive to blood oxygenation level-dependent (BOLD) contrast (Kwong et al. 1992; Ogawa et al. 1992). Whole brain coverage including the entire cerebellum was achieved with 47 3-mm slices aligned to the anterior commissure-posterior commissure plane using automated alignment (van der Kouwe et al. 2005). Structural data included a high-resolution multiecho T1-weighted magnetization-prepared gradient-echo image (multiecho MP-RAGE; van der Kouwe et al. 2008).

For the motor task, subjects performed a blocked-task paradigm consisting of 40-s blocks of active movement interspersed with 18-s blocks of passive fixation. For foot movement, subjects alternated dorsiflexion and plantarflexion of the right foot. For hand movement, subjects individually lifted the right thumb, index finger, and little finger in sequence. For tongue movement, subjects moved the tongue between left, middle, and right positions touching their upper teeth. For each of six runs, six task blocks were embedded for a total of 36 task blocks per participant. All runs began and ended with visual fixation. Before each movement block, a 2-s visual cue informed the subjects to initiate one of three movement types. The fixation crosshair then changed to include a small green circle around its border, indicating to the subjects to continue their movements. At the end of the block, the green circle was removed and subjects passively fixated. The order of movement condition (foot, hand, tongue) was counterbalanced between runs. Subjects practiced the movements before scanning to ensure they understood the directions and were encouraged to maintain a constant rate of repetitive movement throughout movement blocks. To reduce extraneous motion, subjects' legs were supported in a semiflexed position using an ergonomic knee-to-ankle cushion. A piece of tape was attached around the right ankle to limit leg movement during the foot condition. Arms rested on each side of the body with the right hand and wrist supported on a flat foam pad.

Functional imaging parameters were as follows: repetition time (TR) = 3,000 ms, echo time (TE) = 30 ms, flip angle (FA) = 85°, 3 × 3 × 3-mm voxels, field of view (FOV) = 216, and 47 slices collected with interleaved acquisition and no gap between slices. Each functional run in the motor task lasted 6 min 27 s (129 time points). Parameters for the structural scan (multiecho MP-RAGE) were as follows: TR = 2,200 ms, TI = 1,100 ms, TE = 1.54 ms for *image 1* to 7.01 ms for *image 4*, FA = 7°, 1.2 × 1.2 ×-1.2-mm, and FOV = 230.

For the resting-state data used for functional connectivity analysis, subjects were instructed to remain still, stay awake, and keep their eyes open. The acquisition parameters were identical to those described above, except 124 time points were acquired. Resting-state data acquisition is described in more detail in Yeo et al. (2011).

Functional MRI Data Preprocessing

The fMRI data were preprocessed as described in the companion paper (Yeo et al. 2011). Briefly, the first four volumes of each run were discarded to allow for T1-equilibration effects, slice acquisition-dependent time shifts were compensated per volume using SPM2 (Wellcome Department of Cognitive Neurology, London, UK), and head motion was corrected using rigid body translation and rotation using the FMRIB Software Library (FSL) (Jenkinson et al. 2002; Smith et al. 2004). Resting-state data underwent further preprocessing, including low-pass temporal filtering, head-motion regression, whole brain signal regression, and ventricular and white matter signal regression. This regression procedure minimized nonneuronal signal contributions, including respiration-induced signal fluctuations (Birn et al. 2006; Wise et al. 2004), but shifted the distribution of correlations around zero (Vincent et al. 2006), making physiological interpretation of negative correlations tenuous (Fox et al. 2009; Murphy et al. 2009; Van Dijk et al. 2010). In this study, we only interpret positive correlations.

Structural MRI Data Preprocessing and Functional-Structural Data Alignment

The structural data were processed using the FreeSurfer version 4.5.0 software package (http://surfer.nmr.mgh.harvard.edu), which provides automated algorithms for reconstructing surface mesh representations of the cortex from individual subject's structural images and registering each subject to a common spherical coordinate system (Dale et al. 1999; Fischl et al. 1999a, 1999b, 2001; Ségonne et al. 2004, 2007). The cortical surface extraction process is described in Yeo et al. (2011).

The structural and functional images were aligned (Fig. 1, *A* and *B*) using boundary-based registration (Greve and Fischl 2009) within the FsFast software package (http://surfer.nmr.mgh.harvard.edu/fswiki/FsFast). The resting-state BOLD fMRI data were then aligned to the common spherical coordinate system via sampling from the middle of the cortical ribbon in a single interpolation step. A 6-mm full-width half-maximum (FWHM) smoothing kernel was applied to the fMRI data in the surface space, and the data were downsampled to a 4-mm mesh. See Yeo et al. (2011) for details.

Quality Control

Visual inspection of the registered data suggested that accurate representations of the cerebellum and cortical surface were obtained for each subject and that structural and functional image registrations were successful. In addition, the volumetric registration was verified to ensure that the cerebellum was successfully aligned between subjects. Figure 2 shows the results of cerebellar and cortical surface

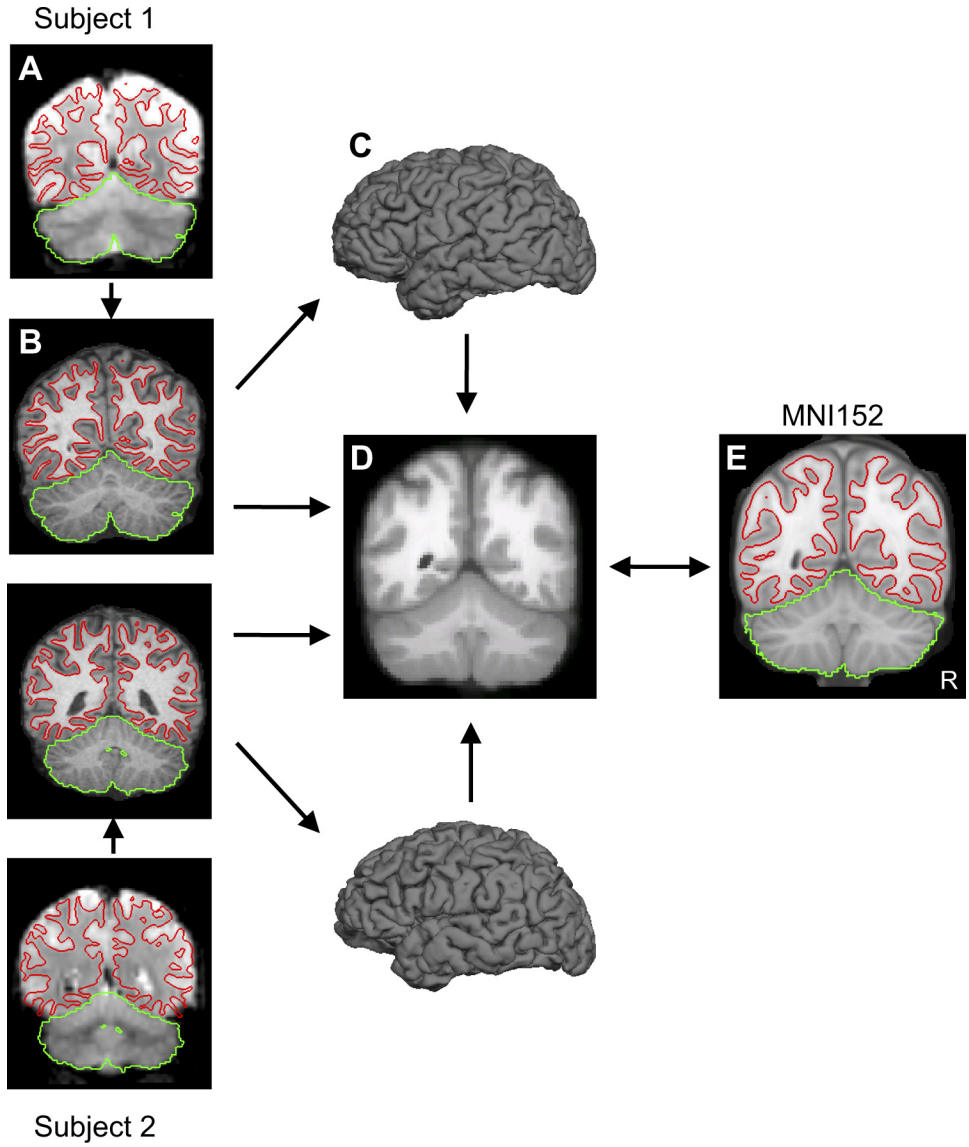

Fig. 1. Hybrid surface- and volume-based registration. For each subject, the T2* images yielding blood oxygenation level-dependent (BOLD)-contrast functional magnetic resonance imaging (fMRI) data (*A*) were registered to the T1-weighted structural data (*B*) in the subject's native space. The cerebral surface and cerebellar boundary were estimated based on the structural data and projected to the BOLD data. The red lines show the estimated inner boundary of the cerebral cortical surface at the gray-white interface. The green line shows the estimated edge of the cerebellum. The cerebral cortical surface was then extracted (*C*) and aligned between subjects using surface-based registration. The T1-weighted structural data were also aligned between subjects using nonlinear volume-based registration (*D*). The surface and volume were then registered to the Montreal Neurological Institute (MNI) atlas space (*E*) for visualization and coordinate reporting.

extraction from the T1 images and T2* to T1 registration of three typical subjects. Intersubject registration is illustrated in Fig. 3.

Hybrid Surface- and Volume-Based Alignment

The resolution of human imaging techniques is sufficient to model functional connectivity across the cerebral cortex as a two-dimensional surface, respecting its topology (Yeo et al. 2011). In principle, the cerebellar cortex could also be modeled as a surface (Van Essen 2002). However, the cerebellar cortex is about one-third the thickness of the cerebral cortex, and the convolutions are sufficiently more complex, making surface-based reconstruction of functional data impractical within the resolution constraints of our present data. For this reason, we adopted a hybrid surface- and volume-based alignment approach. The cerebral cortex was modeled as a surface as described in Yeo et al. (2011), and the cerebellum was aligned using nonlinear volumetric registration.

The volumetric registration algorithm proceeded by jointly deforming the structural volume to a probabilistic template and classifying each native brain voxel into one of multiple brain structures, including left and right cerebellar gray and white matter (Fischl et al. 2002, 2004). The probabilistic template encodes multiple features including *1*) spatial relationships among different anatomical structures (e.g., the cerebrum is dorsal to the cerebellum), *2*) expected MR intensity given the acquisition parameters and intrinsic tissue properties estimated as part of the algorithm (e.g., T1, T2, and T2*), and *3*) spatial variation in MR intensity as a result of spatial variation in intrinsic tissue properties (e.g., T1 is longer in frontal gray matter than primary somatomotor cortex).

The nonlinear deformation is represented by a dense displacement field (i.e., a single displacement vector at each 2-mm isotropic atlas voxel) and is driven by five energy terms: one to encourage smooth deformations, one to minimize metric distortion within each anatomical structure, one to encourage the invertibility of the displacement field, and two terms to maximize the likelihood of the observed image intensity conditioned on the location and identity of the brain structure. The resulting deformation field, together with the correspondence yielded by the structural-functional data alignment discussed above, was used to transform the subject's fMRI data into FreeSurfer nonlinear volumetric space (Fig. 1, *B–D*), thus establishing spatial correspondences between the subject and other subjects that were also brought into this common coordinate system. The resulting volumetric fMRI data were smoothed with a 6-mm FWHM smoothing kernel constrained by the cerebellum mask defined using the FreeSurfer template (Fischl et al. 2002, 2004).

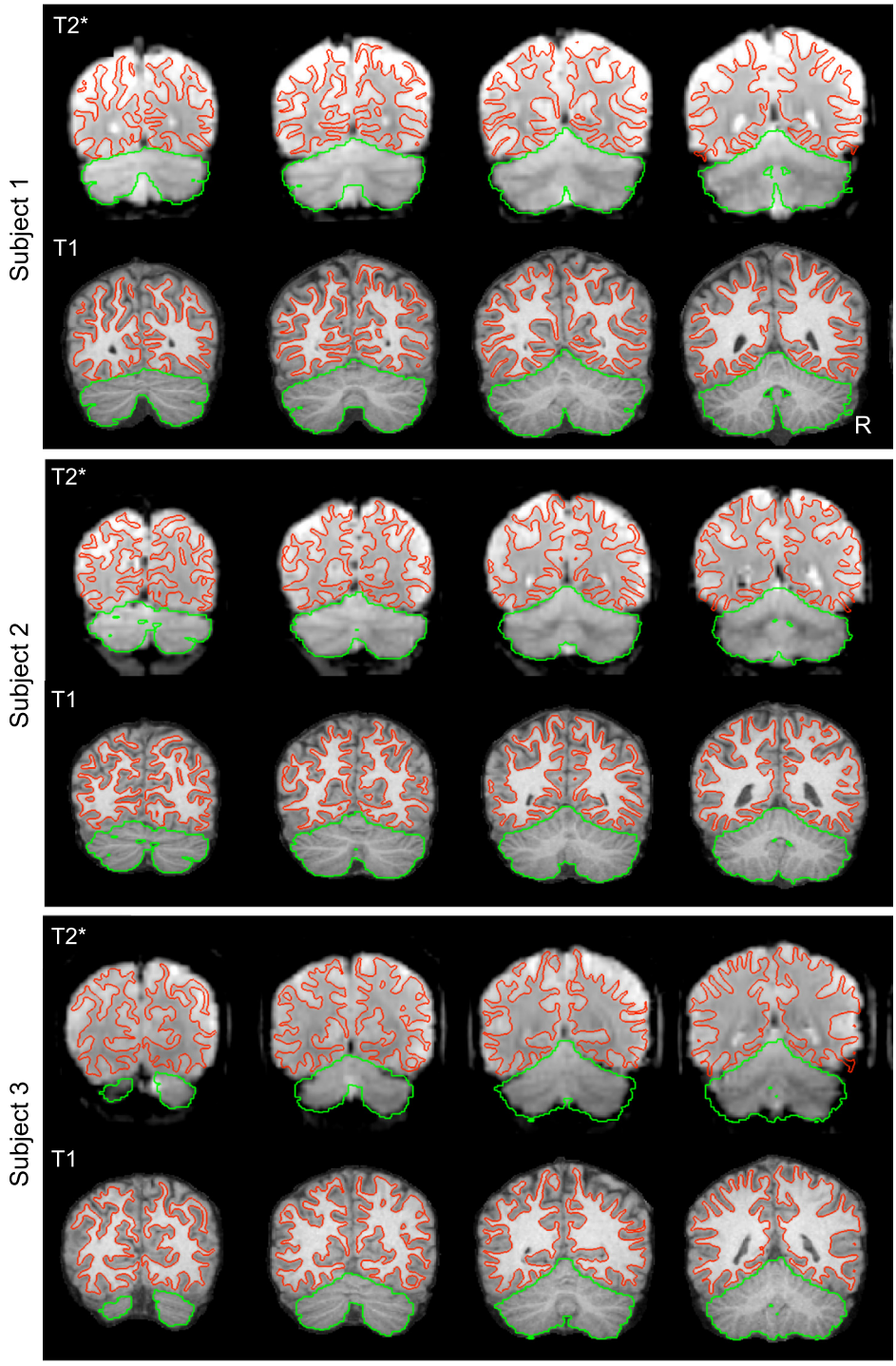

Fig. 2. Examples of within-subject surface and volume extraction. Examples of the extracted cerebral cortex surface and cerebellum boundaries are shown for 3 typical subjects within their native space. The green line shows the estimate edge of the cerebellum tailored to each individual subject's T1-weighted image to illustrate deviations in the T2* images. Imperfections are apparent in the BOLD data, especially in regions prone to susceptibility artifact (e.g., inferior temporal cortex).

Spatial correspondence was established between FSL Montreal Neurological Institute (MNI) space and the FreeSurfer nonlinear volumetric space by running the nonlinear FSL MNI152 template through the FreeSurfer pipeline (Fig. 1, *D* and *E*). All cerebellar analyses were performed in FreeSurfer nonlinear volumetric space. The use of the nonlinear deformation reduces intersubject anatomical variability (Fig. 3).

Mapping Between Surface- and Volume-Based Coordinates and Visualization

At the end of the processing pipeline for a single subject, the transformation from the subject's native space to the FreeSurfer surface coordinate system was estimated, as well as the transformation from the subject's native space to FreeSurfer nonlinear volumetric space (Fig. 1, *A–D*). By concatenating the two transformations and averaging the composed transformations over all 1,000 subjects, we were able to establish spatial correspondence between the FreeSurfer surface and volumetric coordinate systems. Since the spatial correspondence between FSL MNI152 space and FreeSurfer nonlinear volumetric space was also estimated by running the FSL MNI152 template through the FreeSurfer pipeline (Fig. 1, *D* and *E*), this allowed us to obtain spatial correspondences between FSL MNI152 space and FreeSurfer surface space by running the FSL MNI152 template (Fig. 1*E*) through the FreeSurfer pipeline.

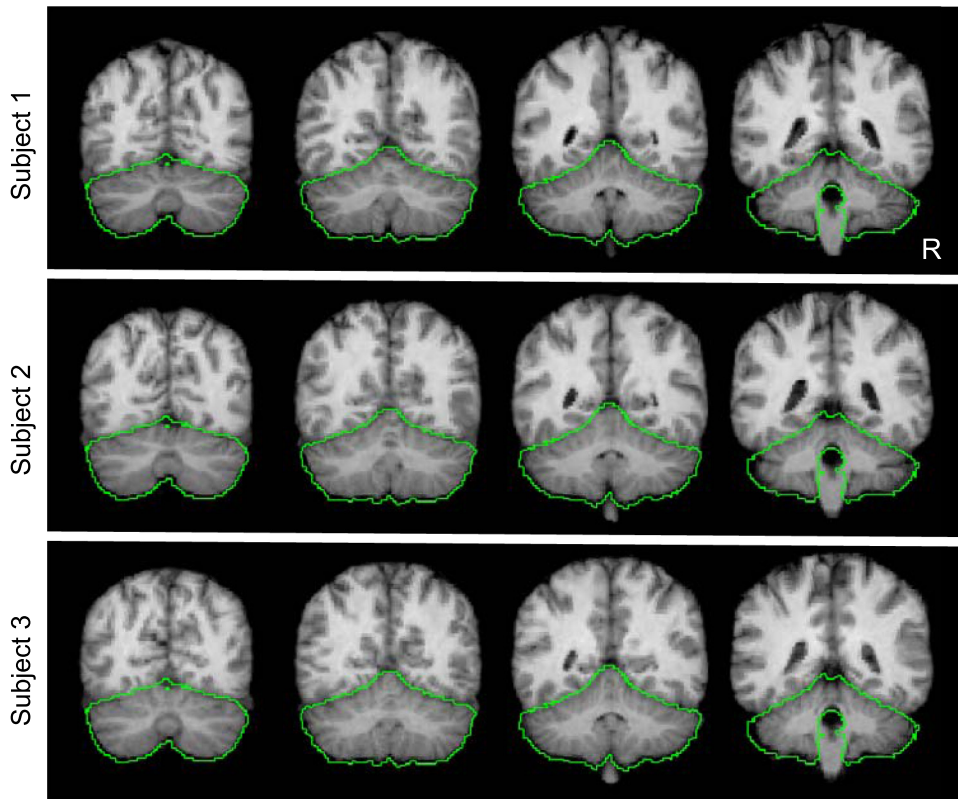

Fig. 3. Examples of between-subject cerebellar alignment. Volumetric alignment is illustrated for the structural data from 3 typical subjects. The green line represents a loose-fitting cerebellar edge estimated from the group template and is displayed identically across the 3 subjects as a reference to illustrate how each individual conforms to the group template. Each subject's cerebellum is well registered in relation to the template. Close examination reveals subtle differences between subjects reflecting alignment errors on the order of a few millimeters. There was no attempt to align the details of the folia between subjects.

These correspondences were used *1*) to compute functional connectivity between the volume and surface representations and *2*) to estimate atlas coordinates using the MNI coordinate framework (Evans et al. 1993) as implemented in the nonlinear FSL MNI152 space (Fonov et al. 2011). For example, signal modulation from a seed region in the cerebellum could be extracted and the functionally correlated surface map computed (see below). The locations of the seed regions could also be described in terms of MNI coordinates even though they were estimated from functional data analyzed within a surface representation.

Although all analyses were performed in FreeSurfer surface and volumetric space, for the purpose of visualization, maps were displayed in the volume using the MNI atlas space and for the surface on the left and right inflated PALS cortical surfaces using Caret software (Van Essen 2005). Cerebellar nomenclature uses the conventions of Larsell (1970) as described in the MRI atlas of Schmahmann et al. (1999, 2000). Diedrichsen et al. (2009) was also relied on to determine fissure and lobule locations.

Regression of Adjacent Cerebral Cortex Signal when Analyzing the Cerebellum

The close physical proximity of the cerebellum to ventral regions of the cerebral cortex results in the blurring of fMRI signal across the cerebellar-cerebral boundary, especially between the visual cortex and the putative somatomotor regions of the cerebellar anterior lobe. Consequently, when no steps are taken to address this issue, functional coupling between neighboring regions of the cerebellum and cerebral cortex is detected that masks functional coupling of the cerebellum to other cerebral regions. To map the full extent of the cerebellar cortex to its principal cerebral targets, we adopted an additional processing step.

The signal arising from the cerebral cortex immediately adjacent to the cerebellum was regressed from the cerebellar signal. This was accomplished by computing masks of left and right cerebral cortex within 6 and 7 mm, respectively, from the cerebellum. The spatial extent of the cerebellum was defined using the FreeSurfer template (Fischl et al. 2002, 2004). The distances used to define the cortical masks were chosen so that the masks wrapped around the adjacent cerebellum. The distances were asymmetric so that the left and right cerebral cortex contributed roughly equally to the regression. For each individual subject, the fMRI signal within the left and right cerebral cortex masks were averaged and regressed from the smoothed fMRI data within the cerebellum. This regression procedure allows mapping of the full surface of the anterior lobe. Because the regression may cause artifactual reduction of true correlation of cerebral regions in the analysis, especially visual cortex, additional analyses were performed with and without regression for key results.

SNR Maps

Temporal SNR of the motion-corrected fMRI time series was computed for each voxel in the subject's native volumetric space by averaging the signal intensity across the whole run and dividing it by the standard deviation over time. The SNR was averaged across runs within subject when multiple runs were available. The SNR was then averaged across the 1,000 subjects from the core data set and displayed in the volume to visualize the SNR of the cerebellum. SNR was good throughout the full extent of cerebellum, with minimal evidence for significant signal loss. However, because the cerebral cortex did possess regions of low SNR, particularly within regions prone to susceptibility artifact, including orbital frontal cortex and inferior portions of the temporal lobe (see Fig. 3 of Yeo et al. 2011), for analyses exploring correlation between the cerebellum and cerebrum, there may be low power to accurately characterize cerebellar regions that are coupled to affected cerebral targets. This issue should be kept in mind when interpreting maps of the cerebellum.

Seed Region Correlation Estimates Between the Cerebellum and Cerebrum

The hybrid surface- and volume-based alignment allowed us to perform region-based analyses between the cerebellum of a subject in

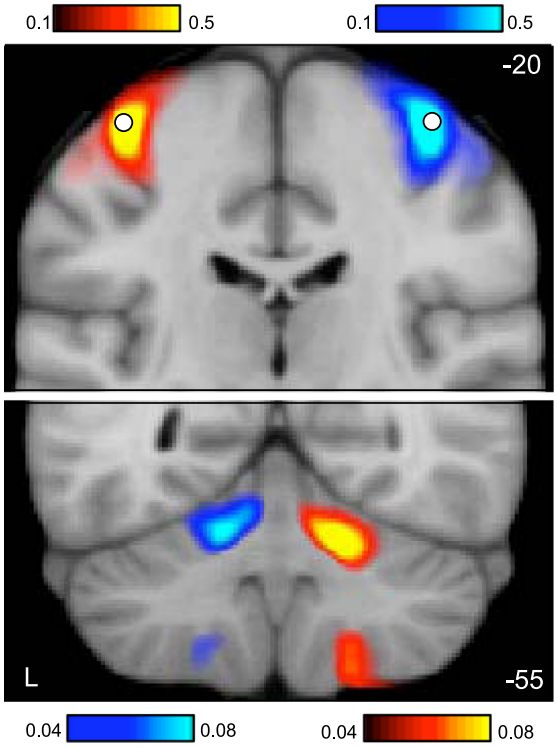

Fig. 4. Functional connectivity of the cerebral motor hand region reveals contralateral somatomotor regions of the cerebellum. Coronal sections (*top*, $y = -20$; *bottom*, $y = -55$) display functional connectivity for the direct contrast between seed motor regions placed in the left and right hand regions of 1,000 subjects (white circles in *top* section display the region locations). Each panel shows connectivity maps for a different coronal section (*top*: $y = -20$ mm, the section containing the hand region of M1; *bottom*: $y = -55$ mm, the section containing the cerebellar hand representation). Red colors display connectivity of the right motor seed region subtracted from the left motor seed region; blue colors display the reverse subtraction. Note the crossed lateralization and double representation in the cerebellum, including the strong primary somatomotor representation in the anterior lobe (*top*) and the slightly weaker secondary representation in the posterior lobe (*bottom*). Color bars indicate the correlation strength [$z(r)$]. The correlation strength near to the seed regions (*top*) is considerably stronger than the distant correlations (*bottom*), necessitating plotting the data using different scales. The left hemisphere is displayed at *left* (neurological convention).

FreeSurfer nonlinear volume space and the cerebrum of the same subject in FreeSurfer surface space. Cerebellar maps for specific cerebral regions were obtained by computing the Pearson's product moment correlation between the surface region's preprocessed resting fMRI time course and the time courses of the voxels within the region of the cerebellum. Cerebral regions included a single surface vertex ($\sim 4 \times 4$ mm) but should be considered spatially more extensive because of the spatial smoothing. Conversely, correlation maps from cerebellar regions were obtained by computing the correlation between the voxel's time course and the time courses of all vertices on the cerebral cortical surface. Cerebellar volumetric regions were also restricted to single voxels ($2 \times 2 \times 2$ mm) and impacted by spatial smoothing.

To obtain group-averaged correlation *z*-maps, the correlation maps of individual subjects were converted to individual subject *z*-maps using Fisher's *r*-to-*z* transformation and then averaged across all subjects in the group. The Fisher's *r*-to-*z* transformation increases normality of the distribution of correlations in the sample. For subjects with multiple runs, the individual subject *z*-maps were first averaged within the subject before submitting to the group average. An inverse Fisher's *r*-to-*z* transformation was then applied to the group-averaged correlation *z*-map, yielding a group-averaged correlation map.

To quantify functional connectivity between regions based on surface vertices and volumetric voxels, Fisher's *r*-to-*z* transformed correlations were computed for each subject within a group. Classical statistical analyses, including *t*-tests and ANOVA, were then performed on the *z*-correlations using Matlab 7.4 (The Mathworks, Natick, MA) or SPSS 18.0 (IBM, Armonk, NY).

Selecting Regions for Functional Connectivity Analysis

Surface and volumetric regions for functional connectivity analysis were selected using criteria appropriate for the purpose of the given analysis. Regional vertices and voxels corresponding to the hand, foot, and tongue representations in the cerebrum and cerebellum were derived based on the analysis of the motor task data set (see *Motor task analysis* for further details). When testing for seed-based confirmation of the resolved cerebellar topography, the confidence maps of the discovery sample were used to derive cerebellar regions to be tested in the replication sample. In addition, we utilized a subset of cerebral regions defined in the companion paper (Yeo et al. 2011) for certain analyses. This subset of regions was selected based on *1*) the meta-analysis of putative human frontal eye field (FEF) coordinates reported in the fMRI literature, *2*) probabilistic histological maps of V1 (Amunts et al. 2000; Fischl et al. 2008) and MT+ (Malikovic et al. 2007; Wilms et al. 2005; Yeo et al. 2010) estimated from 10 subjects mapped to FreeSurfer surface space, and *3*) the estimated cerebral network boundaries and confidence in the discovery sample. Further details can be found in Yeo et al. (2011). If a particular data set was used for defining the region (e.g., discovery sample), functional connectivity was always computed with a different data set (e.g., replication sample), providing unbiased measurement of correlation strength.

Motor Task Analysis

After preprocessing, the task data collected in the 26 subjects were analyzed using the general linear model (GLM), including the three movement conditions as well as fixation as regressors of interest. The onsets of the three movement events were modeled 2 s after the

Table 1. *Locations of seed regions used to quantify specificity of somatomotor networks*

	Left Coordinates	Right Coordinates
Cerebral Cortex		
$M1_F$	−6, −26, 76	6, −26, 76
$M1_H$	−41, −20, 62	41, −20, 62
$M1_T$	−55, −4, 26	55, −4, 26
$S1_F$	−10, −42, 74	10, −42, 74
$S1_H$	−42, −35, 65	42, −35, 65
$S1_T$	−64, −8, 27	64, −8, 27
FEF	−26, −6, 48	26, −6, 48
PrC_v	−50, 6, 30	50, 6, 30
Cerebellum		
Foot	−17, −33, −26	14, −34, −26
Hand	−20, −52, −24	17, −52, −24
Tongue	−18, −61, −21	16, −61, −22

Coordinates represent *x*, *y*, *z* in the atlas space of the Montreal Neurological Institute (MNI). Motor task functional magnetic resonance imaging (fMRI) together with probabilistic histological maps of areas 2 and 4 (Geyer et al. 1996; Grefkes et al. 2001; Fischl et al. 2008) were used to identify $M1_F$, $M1_H$, $M1_T$, $S1_F$, $S1_H$, and $S1_T$ in the left hemispheres (where subscripts F, H, and T indicate foot, hand, and tongue representations) and were reflected across the midline in MNI space to obtain seed regions in the right hemisphere. Motor task fMRI was also used to identify motor seed regions in the right cerebellum. Left frontal eye field (FEF) and ventral precentral cortex (PrC_v) seed regions were obtained from Yeo et al. (2011). Contralateral cerebellar seed regions were obtained by reflection across the midline in the native FreeSurfer volume space, leading to asymmetric MNI atlas coordinates in some instances.

appearance of the cue to account for potential differences in movement initiation/preparation times across the different motor effectors. The duration of each event was set to the remaining duration of each movement block (40 s), and events were modeled with a canonical hemodynamic response function along with its temporal derivative. Regressors of no interest included run means, low-frequency linear trends, and six parameters obtained for correction of rigid body head motion. Contrasts of interest were constructed and analyzed using the SPM2 software package (Friston et al. 1995).

GLM analyses were performed in subjects' native fMRI space. The maps of individual subjects corresponding to each movement contrast were then transformed onto the FreeSurfer surface coordinate system and averaged across subjects. The averaged contrast maps, together with probabilistic histological maps of areas 2 and 4 (Geyer et al. 1996, Grefkes et al. 2001; Fischl et al. 2008), were used to identify peak vertices in M1 and S1 associated with each particular movement.

For the cerebellum, the contrast maps of individual subjects corresponding to hand > foot and foot > tongue were transformed into FreeSurfer nonlinear volumetric space and averaged across subjects. The averaged hand > foot contrast map was used to identify peak voxels associated with either hand or foot movement, whereas the averaged tongue > foot contrast map was used to identify the peak voxel associated with tongue movement. Comparisons of these conditions to fixation produced similar peak coordinates. However, the direct comparison of the two movement conditions additionally removed nonspecific responses in the cerebellum and was therefore preferred (similar to Krienen and Buckner 2009).

Because the task consisted of right hand and foot motion, we selected peaks in the left hemisphere of the cerebrum and in the right hemisphere of the cerebellum. Corresponding seed locations in the contralateral hemispheres were determined by reflecting the peak coordinates across the midline. The bilateral sets of seed regions derived from this procedure were then carried forward to estimate the cerebellar topography of the three motor effectors in the independent resting-state data.

Distribution of Parcellations and Raw Data

A primary result of our analyses is the parcellation of the cerebellum into networks. The parcellations in FreeSurfer space

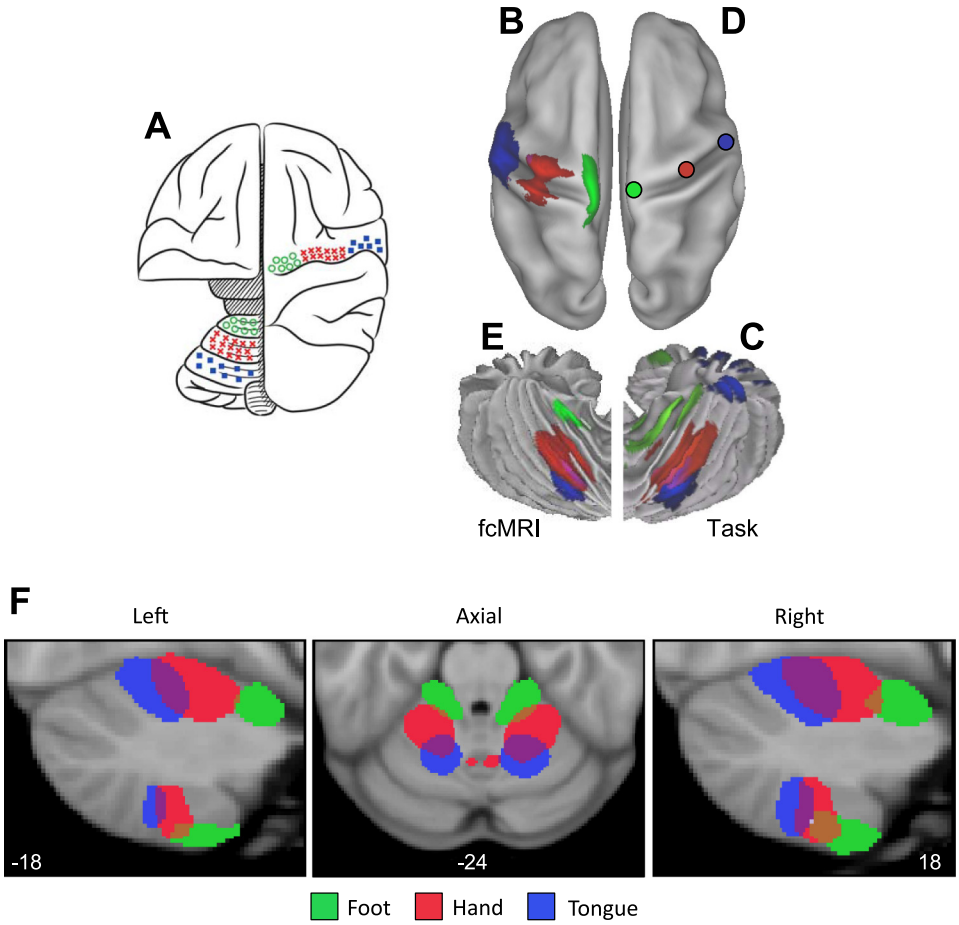

Fig. 5. Functional connectivity reveals inverted somatomotor topography within the anterior lobe of the cerebellum that is comparable to task-evoked estimates. *A*: the cerebral (right hemisphere) and cerebellar (left hemisphere) locations of the hind paw (green), forepaw (red), and face (blue) somatomotor representations in the monkey are known from physiological responses to stimulation. Note that the representation of body space is inverted in the anterior lobe. [Adapted from Adrian (1943).] *B*: the cerebral somatomotor topography evoked by foot (green), hand (red), and tongue (blue) movements as measured by task fMRI in the human. *C*: the inverted somatomotor topography is clearly present in the anterior lobe of the contralateral cerebellum. *D*: right cerebral seed regions were defined based on the task activation data in *B* and reflected across the midline. The seed regions are illustrated for the right hemisphere to show their positions relative to the left hemisphere task data. *E*: the somatomotor map in the cerebellum is displayed based exclusively on functional connectivity MRI (fcMRI) with the contralateral cerebrum. The inverted somatomotor topography is present and similar to the task-based estimates, suggesting functional connectivity can resolve distinct regions of body space within the cerebellum. *F*: 3 views of somatomotor representation within the cerebellum are illustrated. Each estimate comes from a bilateral cerebral region and represents the extent of the functionally coupled response thresholded at $r = 0.04$. Displayed coordinates represent the plane in MNI atlas space. Note that the anterior lobe representation is inverted with the foot anterior to the hand and tongue, whereas the posterior lobe representation is upright with the tongue anterior to the hand and foot.

are available (http://www.freesurfer.net/fswiki/CerebellumParcellation_Buckner2011). Movies of the region-based functional connectivity estimates can be downloaded from http://www.youtube.com/bucknerkrienen. The raw functional MRI data from the 1,000 subjects in the functional connectivity analysis will be made openly available to researchers using the procedures established by the OASIS data releases (Marcus et al. 2007, 2010) and the 1,000 Functional Connectomes Project (Biswal et al. 2010).

RESULTS

Cerebral Motor Regions Show Functional Connectivity with the Contralateral Cerebellum

Subtraction of functional connectivity maps from left and right motor cortex seed regions revealed robust contralateral connectivity in the cerebellum (Fig. 4). Results are shown for analysis of all 1,000 subjects. Coordinates of the motor cortex seed regions are reported in Table 1. The cerebral seed regions were localized within the hand representations. Both the primary and secondary somatomotor representations in the anterior and posterior lobes are evident. Moreover, the functional connectivity is specific to the expected regions of the cerebellum and not broadly throughout the cerebellum.

Functional Connectivity Reveals the Somatomotor Topography of the Cerebellum

Functional connectivity maps from specific cerebral seed regions located in the foot, hand, and tongue representations revealed the expected inverted topography in the contralateral cerebellum (Fig. 5). Results from task-based mapping of cerebellar somatomotor topography (Fig. 5*C*) and the mapping determined exclusively from functional connectivity (Fig. 5*E*) are displayed on the cerebellar surface to allow comparison with each other and with Edgar Adrian's 1943 map of cerebellar topography in the monkey (Fig. 5*A*). The results from the functional connectivity analysis were generally more specific than the task-based activation maps and reveal both the anterior and posterior lobe somatomotor representations (the task-based data did not), but these differences are likely a function of statistical power. The functional connectivity results are based on all 1,000 subjects, whereas the task-based estimates come from 26 subjects who performed active motor tasks.

Figure 5*F* displays the cerebellar somatomotor representation in more detail, including sagittal views to illustrate the reversal of the topographic map ordering between the anterior and posterior lobes. In the anterior lobe, the representation progresses from foot to hand to tongue (inverted representation). In the posterior lobe, the representation progresses from tongue to hand to foot (upright representation).

Figure 6 quantifies the asymmetry of functional connectivity. The task-based activation of the cerebellar hand region was strongly lateralized (subjects moved only their right hands), whereas the tongue region was bilateral, consistent with the bilateral nature of the tongue movement (Fig. 6*A*). The foot lateralization was intermediate. Functional connectivity results (Fig. 6*B*) revealed a similar pattern of asymmetry, with the right cerebral hand region showing strong correlation with the contralateral but not ipsilateral cerebellar regions. The tongue was bilateral, and the foot was intermediate. The 2 × 3 ANOVA including laterality (ipsilateral, contralateral) and motor region (foot, hand, mouth) found a significant interaction

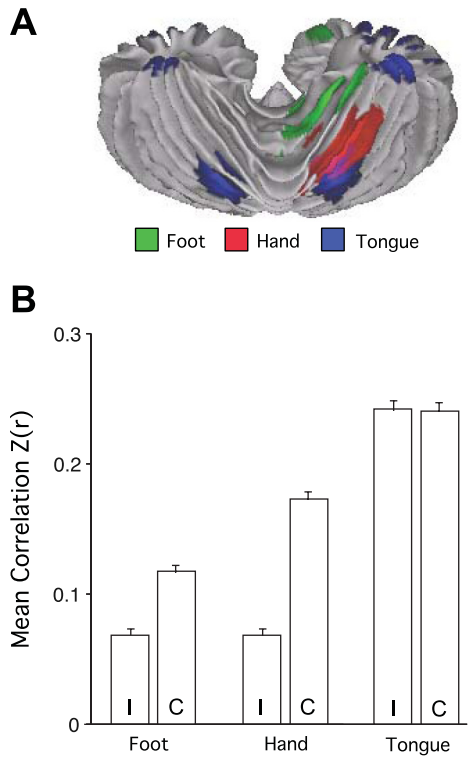

Fig. 6. Asymmetry of somatomotor representations. *A*: the task-based somatomotor representation is displayed for both the left and right hemispheres of the cerebellum. The tongue representation is bilateral, whereas the hand and foot are lateralized. *B*: functional correlation strengths are plotted for the ipsilateral (I) and contralateral (C) cerebrocerebellar region pairs based exclusively on functional connectivity. Error bars display standard error of the mean. Note that the foot and hand are lateralized, with the hand strongly lateralized. The tongue representation is bilateral. The lateralization-by-region interaction is significant ($P < 0.001$), indicating that intrinsic functional correlations show differential lateralization across the body map paralleling the task-based estimates.

($P < 0.001$). Although it is not possible to rule out tongue movements during resting-state scanning, it is nonetheless interesting to note that the asymmetry of cerebrocerebellar functional connectivity parallels task-based patterns of asymmetry.

Functional Connectivity Reveals a Complete Functional Map of the Cerebellum

Having established that functional connectivity can map the topography of cerebellar somatomotor regions with a high degree of specificity, we next mapped the full topography of the cerebellum. The analysis strategy estimated, for each cerebellar voxel, its profile of connectivity to 1,175 cortical regions of interest defined in Fig. 4 of Yeo et al. (2011). A winner-take-all algorithm was adopted such that each cerebellar voxel was assigned to the cerebral network with the most similar profile of connectivity. Thus one limitation of this approach is that the algorithm assumes that there is a single best network. A second limitation is that the cerebral networks are assumed to have a specific topography. Analyses discussed later in this article address both of these limitations.

Figures 7–10 display the main results. Figure 7 displays the reliability of the functional maps of the cerebellum based on connectivity to the 7 major cerebral networks as well as for the

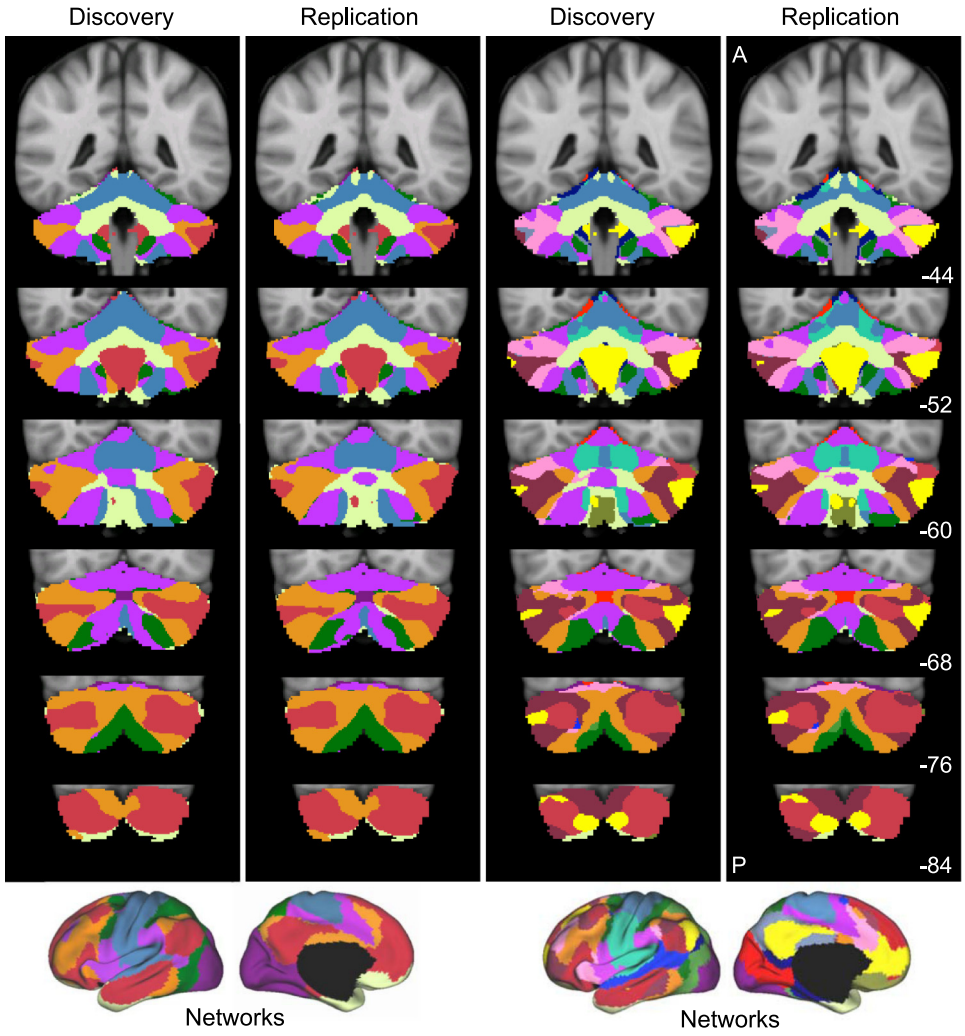

Fig. 7. Reliability of maps of the human cerebellum based on functional connectivity. Every voxel within the cerebellum is colored based on its maximal functional correlation with a cerebral network in the discovery sample ($n = 500$) and replicated in the replication sample ($n = 500$). The 2 *left* columns display the parcellation based on the 7 cerebral networks shown at *bottom left* (from Yeo et al. 2011). For example, the blue regions of the cerebellum include those voxels that are more strongly correlated with the blue cerebral network (involving somatosensory and motor cortices) than any other network. The 2 *right* columns display the parcellation based on the 17 cerebral networks shown at *bottom right* (from Yeo et al. 2011). Note that the discovery and replication maps are highly similar.

17-network estimate (see Yeo et al. 2011). Figure 8 displays a best estimate of the 7-network parcellation of the cerebellum using all 1,000 subjects. Figure 9 displays a best estimate of the finer parcellation using 17 networks. Figure 10 displays the confidence estimates of the parcellations.

Several results are notable. First, expected regions in the anterior and posterior lobes mapped to the somatosensory cerebral network (including lobules IV, V, VI, and VIIIB as shown in blue in Fig. 8). The fine-parcellated cerebral map included two separate networks for somatomotor cortex, one encompassing the hand and foot representations and a second including the face representation. The cerebellar map based on the fine-parcellated solution correctly positioned these topographic regions (colored aqua and blue in Fig. 9). Although unsurprising, these results suggest that our mapping approach is valid. The somatomotor representation did extend into the simplex lobule (HVI). However, HVI largely mapped to cerebral networks associated with premotor cortex and the supplementary motor area.

Second, the majority of the cerebellum mapped to cerebral association networks, including those associated with sensorymotor integration (colored green in Fig. 8), cognitive control (orange), and the default network (red). Cerebellar regions mapped to the cerebral association networks included the entirety of Crus I and II as well as portions of the simplex lobule (HVI), HVIIB, and IX. The cerebellar map generally did not distinguish the vermis from the hemispheres, but rather tended to show topographic specificity along the anterior to posterior axis. However, hints of longitudinal organization can be seen in the coronal sections. For example, the somatomotor regions of the cerebellum are closer to the vermis and do not extend significantly into the hemispheres (e.g., Fig. 8, coronal section $y = -52$).

Third, the cerebellar map did not contain representation of early visual cortex. The fine-parcellated cerebral map contained separate visual networks that roughly encompassed central and peripheral representations of the retinotopically defined visual areas (colored purple and dark red in Fig. 9; see Yeo et al. 2011). Neither of the visual networks displayed functional coupling within the cerebellum.

A final, potentially important observation emerged. As with the somatomotor representation, the cerebellum also possessed a double representation of each cerebral network along its anterior-to-posterior axis, except for the representation of the default network (colored in red in Fig. 8). The representation of the cerebral default network fell at the intersection of the two topographies. That is, the map of the cerebellum contained a full inverted map of the cerebral cortex in its anterior extent and then a second upright representation in its posterior extent. The well-established anterior and posterior lobe representa-

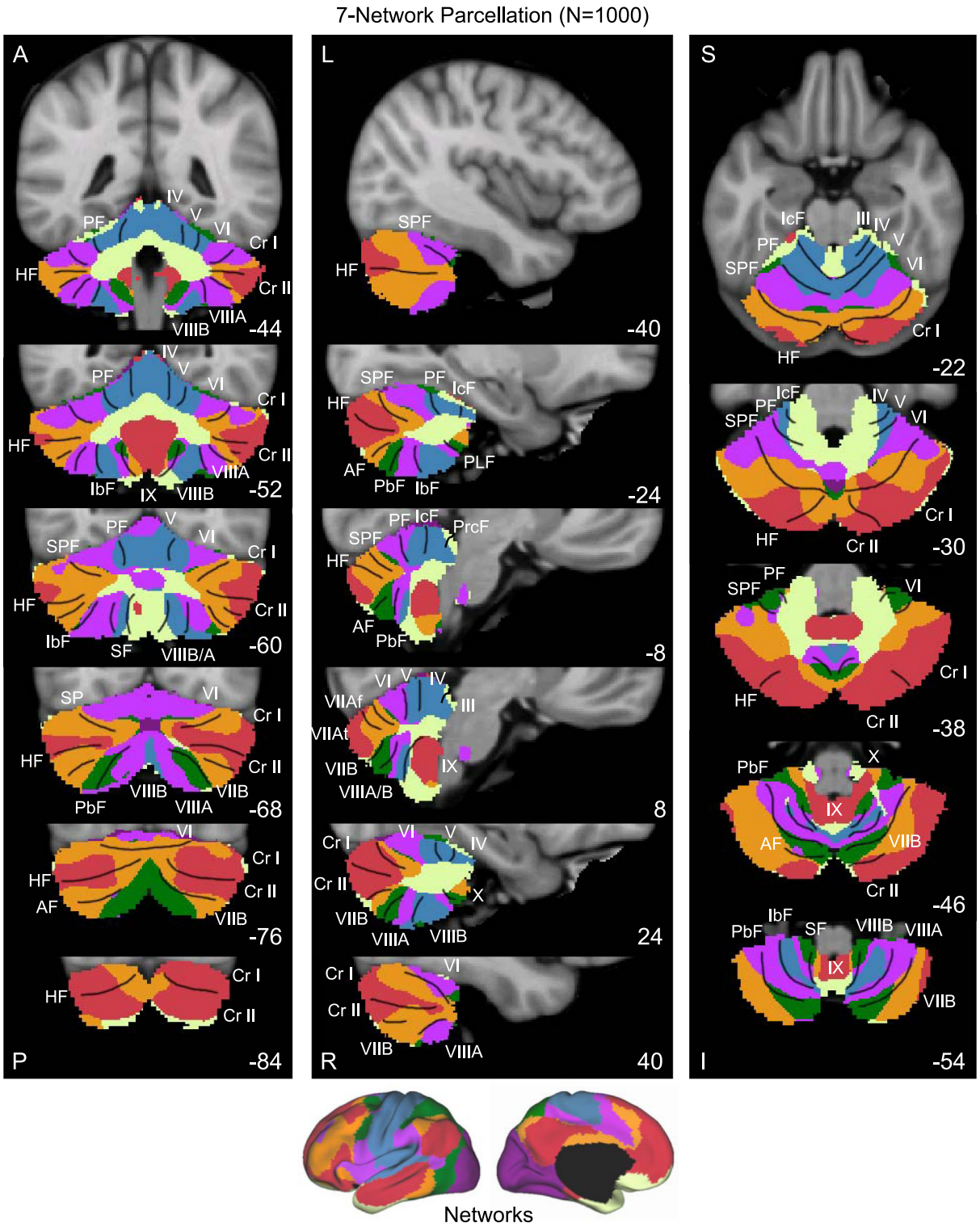

Fig. 8. A map of the human cerebellum based on functional connectivity to 7 major networks in the cerebrum. Every voxel within the cerebellum is colored based on its maximal functional correlation with a cerebral network in the full sample of 1,000 individuals. The map is based on the 7 cerebral networks shown at *bottom* (from Yeo et al. 2011). The sections display coronal (*right*), saggittal (*middle*), and transverse (*left*) images: A, anterior; P, posterior; L, left; R, right; S, superior; and I, inferior. The coordinates at *bottom right* of each panel represent the section level in the MNI atlas space. Major fissures are demarcated on the left hemisphere, and lobules are labeled on the right hemisphere. AF, ansoparamedian fissure; HF, horizontal fissure; IbF, intrabiventer fissure; IcF, intraculminate fissure; PbF, prepyramidal/prebiventer fissure; PF, primary fissure; PLF, posterolateral fissure; PrcF, preculminate fissure; SF, secondary fissure; SPF, superior posterior fissure. Note that this mapping method identifies the correct locations of the primary and secondary somatomotor regions in the anterior and posterior lobes of the cerebellum (shown in blue). The cerebellar hemispheres primarily map to cerebral networks involving association cortex (as exemplified by the networks illustrated in red and orange).

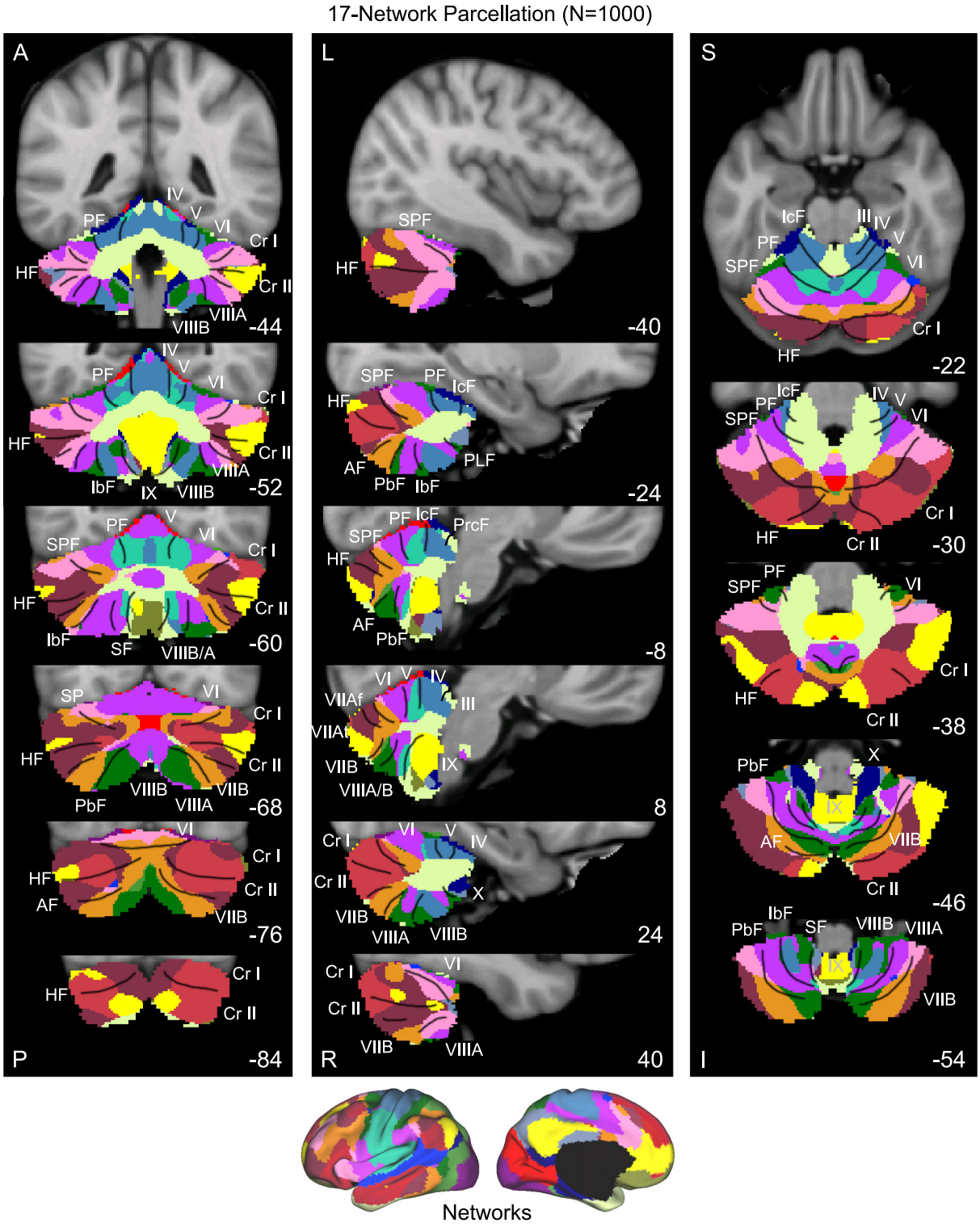

Fig. 9. A fine-parcellated map of the human cerebellum based on functional connectivity to 17 networks in the cerebrum. The format and abbreviations are the same as in Fig. 8 but in this instance are in relation to a finer cerebral parcellation involving 17 networks (from Yeo et al. 2011). These data are from the full sample of 1,000 individuals.

tions of somatomotor cortex may reflect portions of a larger duplicated map of the cerebral cortex within the cerebellum. There is also evidence for a smaller third map in the more posterior extent of the cerebellum. We return to the intriguing possibility that the cerebellum possesses multiple complete maps of the cerebral cortex in the DISCUSSION.

One technical question arises: How many subjects are required to estimate cerebellar topography? Although we could not consistently obtain stable maps of the full cerebellum in individual subjects, the major networks could often be identified (e.g., see the individual subject analyses in Krienen and Buckner 2009). Complete topographic maps that captured

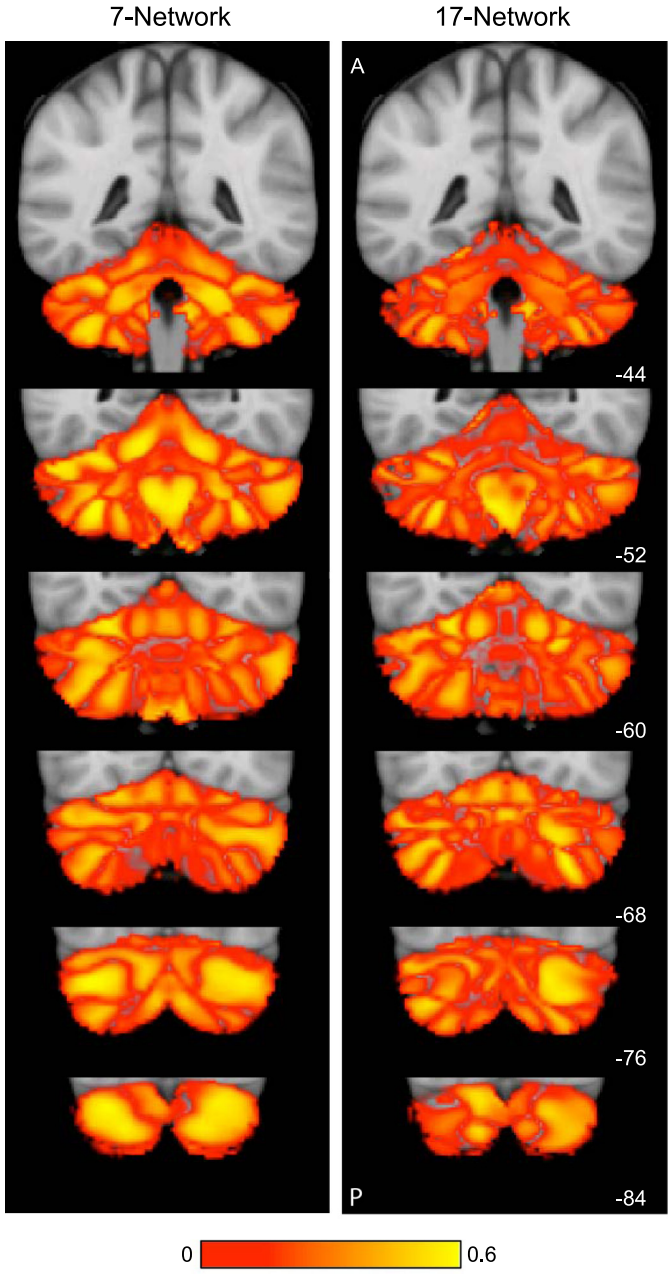

Fig. 10. Confidence of the parcellation estimates. Confidence (silhouette) values for each voxel of the cerebellum with respect to its assigned network are displayed for the 7 (*left*)- and 17-network (*right*) estimates. Estimation of the silhouette values are described in Yeo et al. (2011). Much like the cerebral parcellation (see Yeo et al. 2011), regions near network boundaries are less confident.

much of the topography of the 7-network parcellation could be produced with as few as 10 subjects. Details of the 17-network parcellation, borders between regions, and the edge of the cerebellum near to the cerebral cortex required much larger sample sizes to stabilize.

The Cerebellum Is Proportionately Mapped to the Cerebrum with a Few Exceptions

The analyses above resulted in a complete map of the anterior and posterior cerebellar lobes. Such a map provides an opportunity to ask quantitative questions about the relation between cerebellar and cortical mapping: Is the size of a cerebellar region dedicated to a network proportionate to its representation in the cerebral cortex? And what is the relative proportion of the cerebellum dedicated to putatively motor vs. nonmotor cerebral networks? To address these questions, we calculated the percentage of the cerebral surface area occupied by each of the networks from the 17-network parcellation (from all 1,000 subjects). We next calculated the volume of the cerebellum dedicated to that same network after masking the cerebellum to include only gray matter. The assumption is that the cerebellar volume of a region is a reasonable proxy for the cerebellar cortical area (which could not be computed due to resolution limitations). Figure 11 plots the results.

Results showed that, in general, there is a strong relation between the cerebral surface area and its representation in the cerebellum; the relation appears to be roughly homotopic. Networks with the largest percentages of the cerebrum tend to have the largest cerebellar representations. However, there are exceptions. Some regions have no detectable representation in the cerebellum, including early visual (networks 1 and 2) and auditory (network 14) networks.

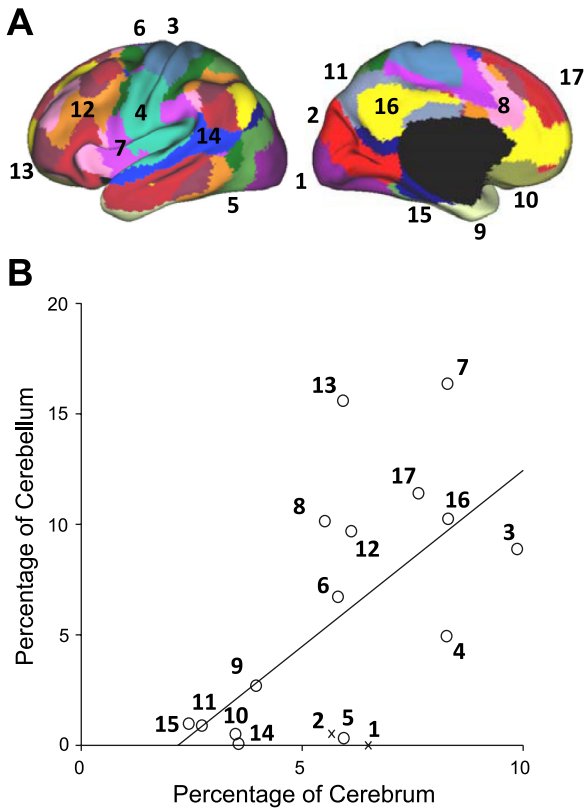

Fig. 11. Quantitative relation between the extent of cerebral and cerebellar cortices dedicated to distinct functional networks. The percentage of cerebral surface area dedicated to each network is plotted against the volumetric percentage of the cerebellar gray matter dedicated to the same network. These estimates are based on 1,000 subjects. *A*: the reference map is illustrated with numbers identifying the estimated networks. *B*: the quantitative relation is plotted with the best-fit line. Open circles represent individual networks, with their networks labeled by numbers corresponding to *A*. The x's represent networks whose cortical partners are used in regression (e.g., visual cortex), possibly biasing analysis (see Fig. 12 for elaboration).

Primary Visual Cortex and Auditory Cortex Are Not Represented in the Human Cerebellum

Exceptions to the general trend for cerebral areas to have proportionate representations in the cerebellum were found for visual and auditory cortices. However, these analyses have limitations. First, because the cerebellar voxels are assigned to their most strongly correlated cerebral network, it remains possible that correlations are present but that they are overshadowed by correlations to other networks. Second, to reduce induction of artifactual correlations in the cerebellum from immediately adjacent occipital cortex, the signal from these regions was regressed out (see METHODS). Thus it is possible that the extent of the cerebellum coupled to visual cortex is underestimated.

We conducted analyses to address these issues. Regions were defined within the central and peripheral estimates of V1 based on histology. Coordinate locations of the visual seed regions are reported in Table 2. Functional connectivity with each of these cerebral regions was then mapped within the cerebellum for the full sample of 1,000 subjects. The map was computed for each visual region in isolation without reference to other cerebral networks. Furthermore, fcMRI maps were computed with and without regression of signal from occipital cortex near to the cerebellum. Results are shown in Fig. 12. No evidence for functional coupling of central or peripheral V1 with the cerebellum was detected beyond coupling of cerebellar cortex immediately adjacent to visual cortex. The same analysis was repeated for a region at or near auditory cortex (Fig. 12; *x*, *y*, *z* MNI coordinate = −51, −45, 11). Again, no evidence was found for functional coupling within the cerebellum.

Table 2. *Locations of seed regions used to quantify specificity of association networks*

	Left Coordinates	Right Coordinates
Cerebral cortex		
$M1_H$	−41, −20, 62	41, −20, 62
$S1_H$	−42, −35, 65	42, −35, 65
FEF	−26, −6, 48	26, −6, 48
PrC_v	−50, 6, 30	50, 6, 30
6vr+	−55, 6, 11	55, 6, 11
PFC_{da}	−31, 39, 30	31, 39, 30
$V1_p$	−16, −74, 7	16, −74, 7
$V1_c$	−13, −100, −8	13, −100, −8
MT+	−45, −72, 3	45, −72, 3
PCC	−3, −49, 25	3, −49, 25
PFC_d	−15, 42, 46	15, 42, 46
STS	−55, −10, −16	55, −10, −16
PFC_{la}	−41, 55, 4	41, 55, 4
PFC_{lp}	−45, 29, 32	45, 29, 32
Cerebellum		
Ventral attention	−31, −62, −21	30, −62, −21
Frontoparietal control	−42, −73, −26	39, −72, −27
Default network	−32, −79, −31	29, −78, −32
Dorsal attention	−6, −76, −43	9, −75, −43

Left cerebral cortical seed regions were obtained from Yeo et al. (2011) except PFC_d, which was selected from the high-confidence default network region in the dorsal prefrontal cortex in the discovery data set. Left cerebellar seed regions were selected from each association network based on the discovery data set, using the confidence map as a guide. Contralateral seed regions were obtained by reflection across the midline. M1, primary motor cortex; S1, somatosensory cortex; V1, visual cortex; PCC, posterior cingulate cortex; STS, superior temporal sulcus. Labels for the regions within the cerebellum correspond to the network names as commonly used in the human neuroimaging literature and should be used as heuristics (see Yeo et al. 2011 for discussion). Alternative names and variations exist. For example, the ventral attention network is most likely an aggregate of closely adjacent networks variably referred to as the ventral attention, salience (Seeley et al. 2007), and cingulo-opercular (Dosenbach et al. 2007) networks. Similarly, the default network can be meaningfully fractionated (e.g., Andrews-Hanna et al. 2010).

Quantitative Measurement of Cerebrocerebellar Circuits Demonstrates Specificity

Analyses up to this point focused on cerebellar maps based on estimating the primary functionally coupled targets for defined cerebral networks. Such analyses assume that the topographies of cerebral networks are respected by the cerebrocerebellar connectivity patterns. If a region in the cerebellum correlated with a fundamentally different pattern in the cerebrum, it would still be assigned to the best-fitting network and the discrepancy would go undetected. To address this issue, we conducted a series of analyses with two goals. First, the full cerebral connectivity patterns were mapped for specific cerebellar seed regions. Such maps are not bound by assumptions about the cerebral topography and thus serve to independently verify whether the networks described above accurately represent cerebrocerebellar circuits as measured by functional connectivity. Second, functional connectivity was measured between multiple seed regions within the cerebellum and the cerebrum to quantitatively explore specificity of cerebrocerebellar circuits. As with earlier analyses, we began by focusing on somatomotor cortex because of its established properties. After analysis of somatomotor cortex, we extended the procedures to cerebrocerebellar circuits linked to association areas.

Figure 13 displays results for somatomotor cortex. Seed regions were placed along the right somatomotor representation of the cerebellar anterior lobe within the estimated foot, hand, and tongue representations. The cerebral functional connectivity maps were then computed for each topographically specific set of seed regions (Fig. 13*A*). Results revealed that, at a map level, the functionally correlated cerebral regions are restricted to the somatomotor cortex and march from the midline to lateral surface as expected based on known topography. The cerebral topography appeared specific. See http://www.youtube.com/bucknerkrienen for animation of this observation.

Somatomotor cortex. Region-based correlations were next computed to quantify these observations. Functional connectivity strengths between each cerebellar seed region and the entire set of cerebral somatomotor regions were computed and plotted in polar form (Fig. 13, *B* and *C*). Functional connectivity strengths were computed between the contralateral cerebral and cerebellar regions and averaged across the hemispheres. The polar plot displays functional connectivity strength from −0.05 to 0.25. Note that the coupling between the cerebellum and cerebral cortex is preferential to the representations of the relevant body part. Moreover, none of the cerebellar regions associated with the primary somatosensory representations are coupled to the putative human FEF region. These results quantitatively demonstrate a high level of specificity between the cerebellum and cerebral partners in somatomotor cortex.

Association cortex. We next generalized the approach described above to explore four regions of the cerebellum

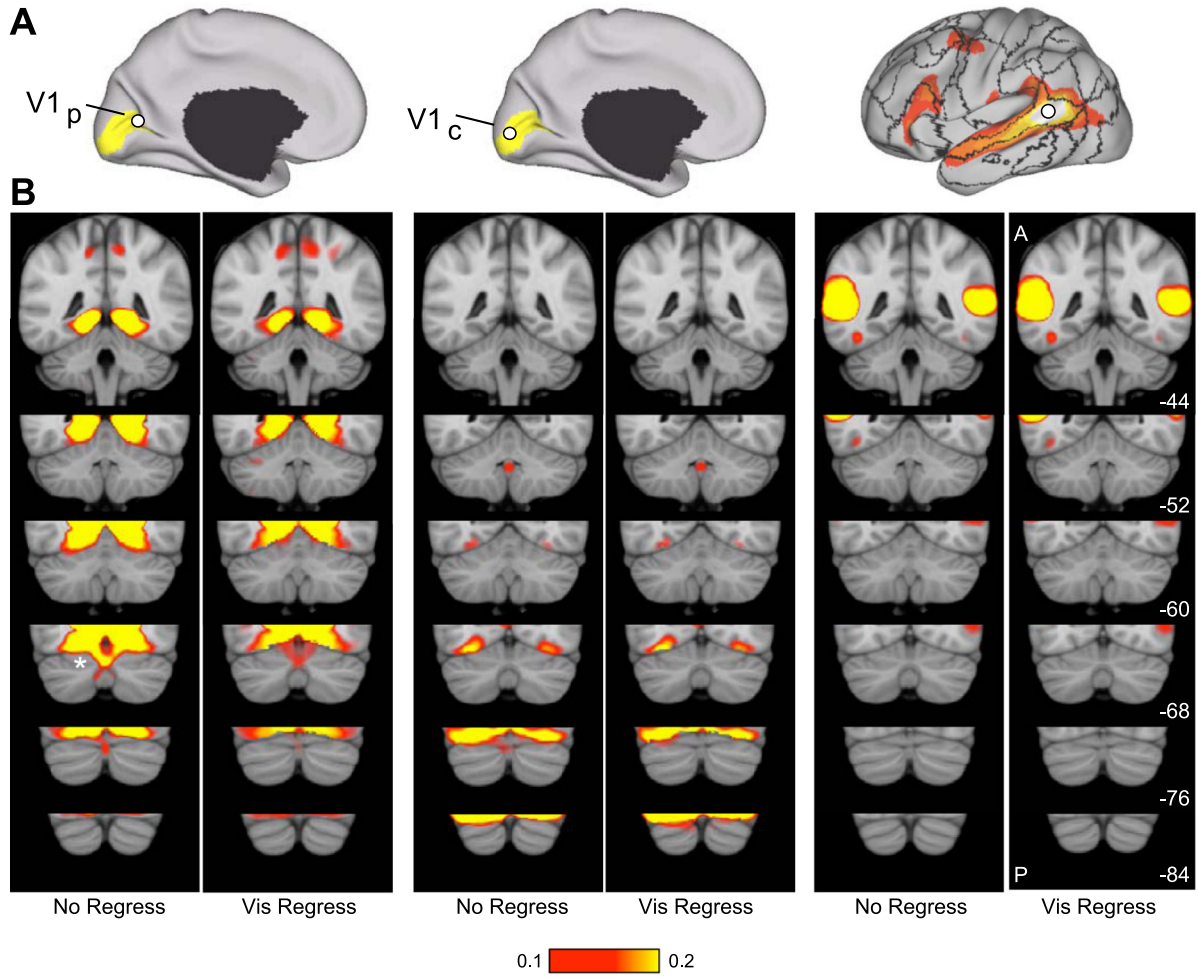

Fig. 12. Evidence that the human cerebellum does not show functional connectivity with primary visual and auditory cortices. Functional connectivity between the primary visual cortex and the cerebellum was examined in detail. *A*: 2 primary visual cortex regions were selected based on postmortem histological estimates on V1 projected onto the cortical surface reference. $V1_p$, peripheral representation of V1; $V1_c$, central representation of V1. Shaded yellow areas represent the surface projection of histologically estimated V1. A region near auditory cortex (*right*) was also selected. *B*: functional connectivity maps for each seed region without (no regress) and with regression of the visual signal near the cerebellum (vis regress). Regression was removed to ensure that the map is not underestimating the representation of visual or auditory regions within the cerebellum. There is no evidence for representation of primary visual or auditory cortices within the cerebellum except for cerebellar cortex just adjacent to visual cortex (marked by an asterisk in leftmost column).

coupled to cerebral association cortex (Fig. 14). Again, the cerebral maps derived from functional connectivity with cerebellar seed regions reveal specific topography. Each set of cerebellar seed regions mapped to a distinct set of distributed cerebral regions. Of importance, the cerebral regions largely fall within the networks as defined in Yeo et al. (2011). For example, cerebellar seed regions on the border of Crus I/II (Fig. 14*A*) demonstrate functional connectivity with distributed cerebral regions linked to the default network, including the posterior cingulate, the lateral temporal cortex, the inferior parietal lobule, and an extended region along medial prefrontal cortex. By contrast, distinct cerebellar seed regions anterior in Crus I (Fig. 14*B*) demonstrate functional connectivity with dorsolateral prefrontal cortex, the rostral portion of the inferior parietal lobule, and a frontal midline region bordering presupplementary motor area and the anterior cingulate.

The four cerebrocerebellar circuits involving association cortex were quantified. Distributed cerebral regions were selected as shown in Fig. 15*A*. The correlation strengths between the cerebellar regions and the distributed cerebral regions are displayed in Fig. 15, *B–E*. Much like the selectivity observed for the somatomotor regions (Fig. 13), the cerebrocerebellar circuits involving association cortex also display selectivity. These results support the hypothesis that cerebrocerebellar circuits arising from distinct cerebellar regions are selective for separate and distributed cerebral networks. The selectivity does not divide broad lobar regions of the cerebral cortex (e.g., the frontal lobe vs. the parietal lobe), but rather maps to distributed regions that are components of distinct functionally coupled cerebral networks (Yeo et al. 2011).

DISCUSSION

The results revealed both expected and novel organizational properties of the human cerebellum. Confirming known functional anatomy, somatomotor representations of body space were observed in the anterior and posterior lobes that were topographically mapped and preferentially contralateral with respect to the cerebrum. Somatomotor regions occupied only a small portion of the cerebellum. The majority of the human

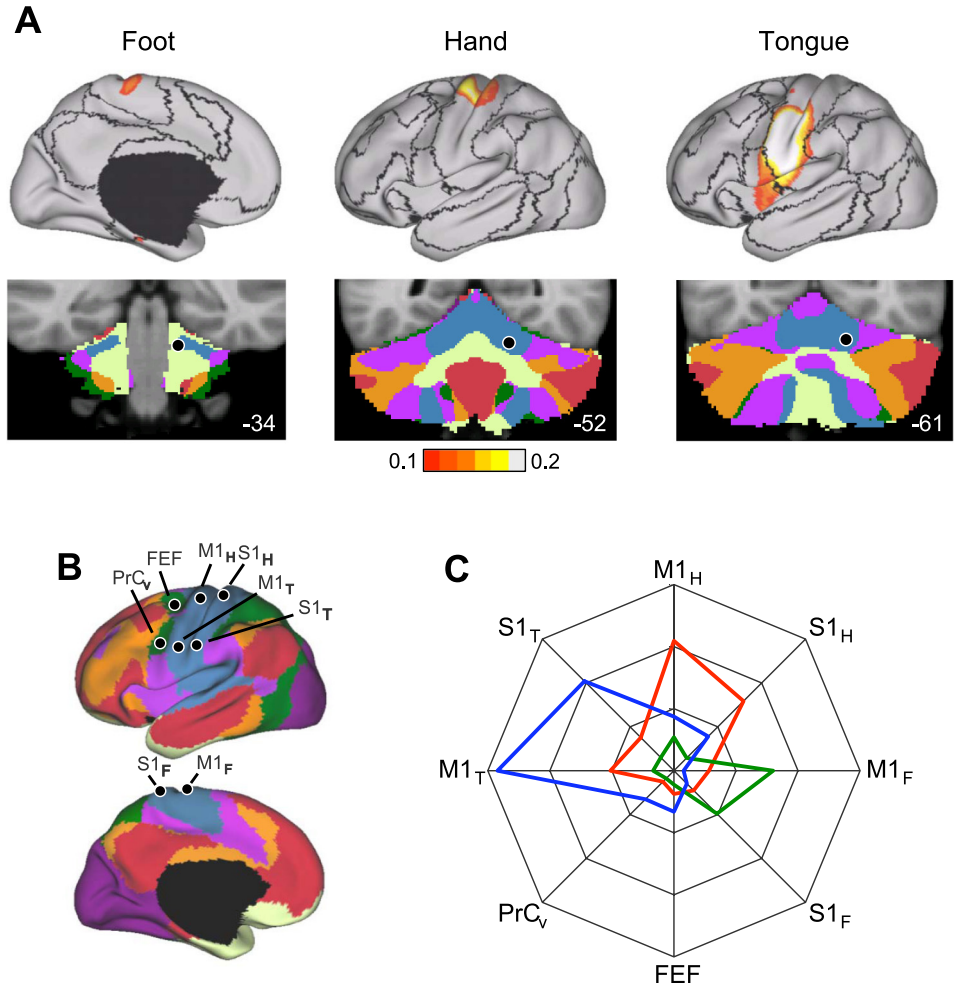

Fig. 13. Cerebrocerebellar circuits involved in somatomotor networks demonstrate topographic specificity. *A*: left cerebral cortex connectivity maps are shown for right seed regions within the estimated foot, hand, and tongue representations of the anterior lobe of the cerebellum. The surface maps show the entirety of the functional connectivity pattern (threshold $r = 0.1$). The dark lines on the cortical surface represent the boundaries of the 7 cortical networks, plotted for reference. The locations of the cerebellar seed regions are shown below each map. *B*: left cerebral regions are displayed that were used for quantitative assessment of specificity. Right cerebral regions obtained from reflecting left cerebral regions across the midline are not shown. PrC_v, ventral precentral cortex; FEF, frontal eye field. Subscripts H, F, and T indicate hand, foot, and tongue representations in M1 and S1 cortex. *C*: quantitative measures of functional connectivity strength are plotted in polar form for cerebellar anterior lobe seed regions linked to the foot (green line), hand (red line), and tongue (blue line) representations. Functional connectivity strengths were computed between contralateral cerebral and cerebellar regions and averaged across the hemispheres. The polar scale ranges from $r = -0.05$ (center) to $r = 0.25$ (outer boundary) in 0.1-step increments.

cerebellum mapped to cerebral association cortex in an approximately homotopic manner: the largest cerebral networks were associated with the most extensive representations in the cerebellum. When the full cerebellar topography was examined comprehensively, an unexpected observation emerged that included both the somatomotor and association representations. The cerebellum possesses three distinct maps of the cerebral cortex. The primary map begins with an inverted somatomotor representation in the anterior lobe and then progresses posteriorly with sequential representations of distinct premotor and association networks. The topography inverts near Crus I/II, forming a mirror-image secondary map of the full cerebrum in the posterior lobe. A final inversion occurs, yielding a tentative tertiary map in the most posterior zone near lobule IX. We discuss these findings in relation to prior studies of cerebellar organization, as well as caveats and ambiguities associated with using functional connectivity as a mapping tool.

Somatomotor Representation in the Human Cerebellum

Using functional connectivity, the primary and secondary somatomotor representations were detected in the anterior and posterior lobes of the cerebellum (Fig. 5). The locations were consistent with expectations based on monkey (Adrian 1943) and cat physiology (Snider and Stowell 1944) and prior task-based estimates of cerebellar somatomotor topography in the human (e.g., Grodd et al. 2001; Wiestler et al. 2011). The anterior representation was inverted, progressing from foot to hand to tongue, forming an upside down "'homunculus." The posterior representation revealed a mirror-image, upright representation. The symmetry of functional connectivity was not uniform across the topographic representation. The hand representation was significantly more lateralized than either the foot or tongue representations (Fig. 6), paralleling the observation of Yeo et al. (2011) that the hand representation shows the weakest functional coupling with the opposite hemisphere. One possibility is that intrinsic functional coupling reflects the functional independence of the right and left hands. Anatomical studies in the monkey have observed variation in the projection patterns for different topographic zones of M1, with the hand and foot representations absent interhemispheric projections (Pandya and Vignolo 1971).

Two further observations are notable. First, the primary somatomotor representation in the anterior lobe extends just beyond the primary fissure and then stops. The regions of the cerebellum posterior to the primary somatomotor representation near HVI are associated with a cerebral network including premotor regions that do not possess a discernable motor topography by our analyses. Schlerf et al. (2010) recently hypothesized a somatomotor representation in this region that supports complex motor movements. Our data suggest that such a representation, if it exists, is not topographically coupled to the topography of primary motor

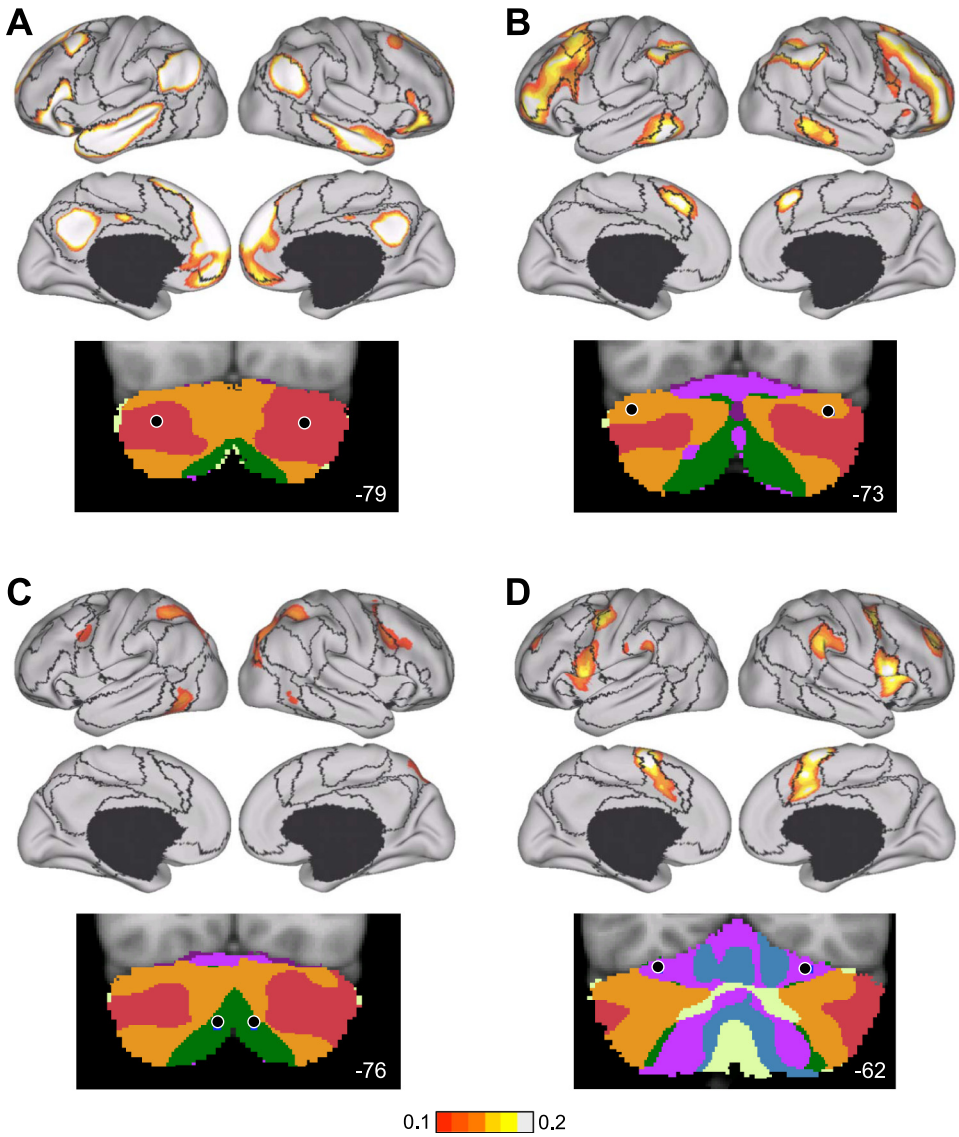

Fig. 14. Evidence for specificity of cerebrocerebellar circuits involving association cortex. The strategy for exploring and quantifying the specificity of somatomotor circuits in Fig. 13 is generalized to distributed regions of association cortex. *A–D* each display the whole brain cerebral surface connectivity pattern for a specific set of bilateral cerebellar seed regions (shown below each map). Cortical maps are displayed based on functional connectivity with contralateral cerebellar regions. Note that separate regions of the cerebellum are selectively correlated with distinct cerebral association networks, including those linked to higher level cognition.

cortex. In our data, the cerebellar region examined by Schlerf et al. is functionally coupled to cerebral regions that participate in motor control (premotor regions) as well as response selection (see Yeo et al. 2011 for discussion). It will thus be interesting in the future to examine the topography of these premotor structures using complex motor movements such as sequences of extension and flexion across digits. Second, the secondary motor representation in the posterior lobe was located at or near lobule VIII. It did not continue into the most posterior extent of the cerebellum including lobule IX. Thus, in addition to needing a functional account of the organization of the extensive intermediate portion of the cerebellum between the somatomotor representations including Crus I and II, the somatomotor maps also leave unexplained the most posterior region near IX.

Representation of Cerebral Association Cortex in the Human Cerebellum

The majority of the human cerebellum is functionally coupled to cerebral association areas. Of particular interest are cerebral networks associated with cognitive control (the orange network in Fig. 8) and the default network (the red network in Fig. 8). Almost one-half of the human cerebellum targets these two cerebral networks, including all of Crus I and II. These networks have been extensively studied in the human literature for their potential role in higher level cognition, including remembering and planning. Prior fcMRI studies have noted functional coupling of these cerebral networks to the cerebellum (Habas et al. 2009; Krienen and Buckner 2009; O'Reilly et al. 2010). The present results provide a more complete map.

By comprehensively mapping the cerebral cortex and also the cerebellum, we were able to quantitatively explore the relation between the extent of the cerebral representation of a network and its volume in the cerebellum (Fig. 11). A roughly linear relation emerged, but exceptions were noted. In general, the extent of the cerebellum dedicated to a network was predicted by the size of the network in the cerebral cortex. If anything, there was an overrepresentation of association networks in the cerebellum. However, the exact details of the relation may be biased, because some regions of the cerebral cortex had poor SNR, including the

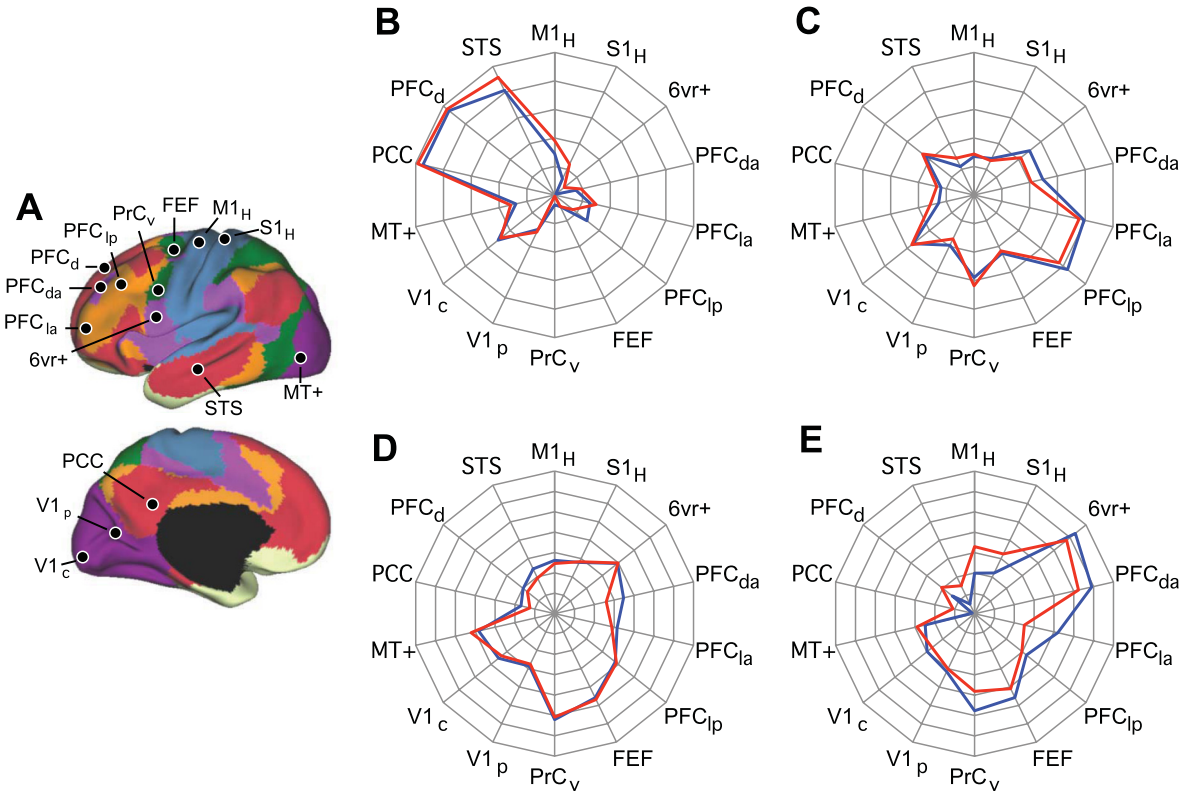

Fig. 15. Quantitative evaluation of the specificity of cerebrocerebellar circuits involving association cortex. *A*: reference regions used for quantitative analysis of association cortex. PCC, posterior cingulate cortex; PFC, prefrontal cortex; STS, superior temporal sulcus. *B–D*: polar plots of functional connectivity strength for each of the seed regions from Fig. 14. Note that each polar plot has a distinct connectivity profile. The red lines display functional connectivity strength between the left cerebellar seed regions and right cerebral cortex seed regions, and the blue lines display the contralateral pairings. The similarity between the red and blue lines shows that the coupling profiles are reliable between the hemispheres. For *B* and *C*, the polar scale ranges from $r = -0.2$ (center) to $r = 0.3$ (outer boundary) in 0.1-step increments. For *D* and *E*, the polar scale ranges from $r = -0.15$ (center) to $r = 0.2$ (outer boundary) in 0.05-step increments.

inferior temporal cortex and orbital frontal cortex (see Fig. 3 of Yeo et al. 2011). Cerebellar regions that are functionally correlated to these regions may be underestimated.

One inconsistency with prior findings concerns the characterization of the cerebellar regions that couple to the default network. Replicating the findings of Krienen and Buckner (2009) but different from those of Habas et al. (2009), we observed that the major region of the cerebellum coupled to the default network is within Crus I/II (the red network in Fig. 8). This region is surrounded by a representation of the frontoparietal control network (the orange network in Fig. 8) and is distinct from the region mapped to IX. Several analyses confirmed this topography. Examining the cerebral map generated from examining functional connectivity for a small seed region placed within Crus I revealed a near-complete map of the default network (Fig. 14*A*). Quantitative analysis demonstrated that coupling to the default network is selective (Fig. 15*B*) and distinct from the frontoparietal control network (Fig. 15*C*). Thus we are confident that the large region in Crus I/II is the major cerebellar region coupled to the default network. The observation that this cerebellar region is surrounded by a distinct association network on both its anterior and posterior borders may have led to the difficulty in detecting its presence in some prior analyses. In the next section, a hypothesis is offered that may account for this peculiar organizational feature.

Cerebellar Topography Consists of Multiple, Inverted Representations of the Cerebrum

The cerebellum, like the cerebral cortex, is a two-dimensional sheet of cortex (Van Essen 2002). Unlike the cerebral cortex, the cerebellum's histology is essentially invariant throughout cortex and has no discernable areal boundaries (Ito 1984). The well-established maps of body space in the anterior and posterior lobes suggest that the cerebellum has multiple, orderly topographic representations that presumably arise from anatomical connectivity patterns. The historical puzzle has been to account for the remaining regions of the cerebellum between the established somatomotor maps (Manni and Petrosini 2004). The present results suggest a parsimonious explanation that links both the known topography of the somatomotor representations and the newer results that map the intervening regions to multiple cerebral association networks.

The seemingly complex organization of the cerebellum can be accounted for by the hypothesis that the cerebellum possesses a complete map of the cerebral cortex that begins in the anterior lobe and extends into Crus I/II, and then a second mirror-image map that begins in Crus I/II and extends through the posterior lobe. Figure 16 presents sagittal sections from the left cerebellum that best illustrate this organization. The two cerebellar maps do not represent only the somatomotor cerebral cortex, but rather map an orderly

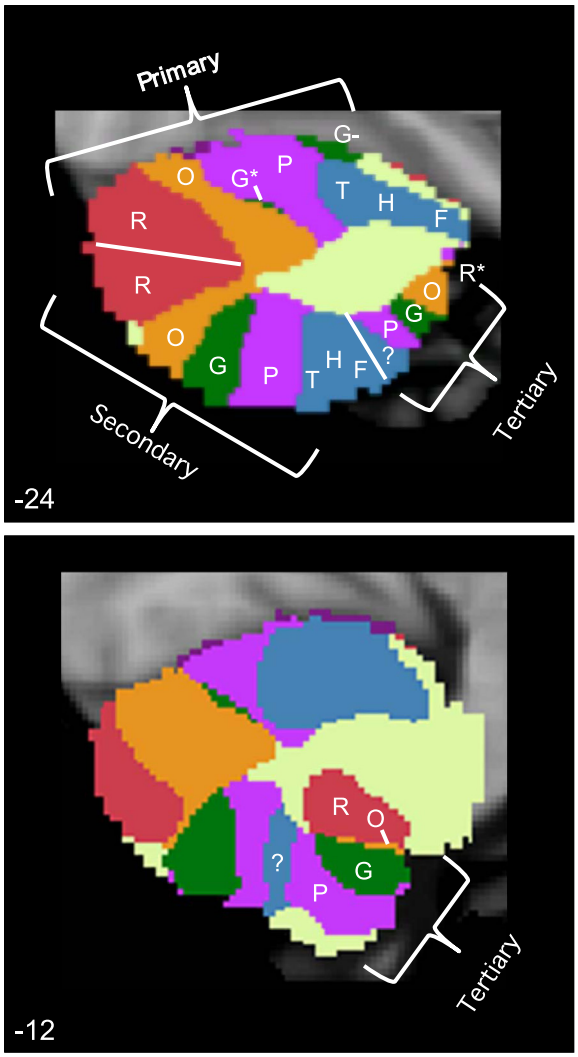

Fig. 16. The cerebellum possesses multiple representations of the cerebral cortex. The topographic orderings of the cerebral networks are illustrated for 2 sagittal sections of the left cerebellum ($x = -24$ and $x = -12$). The parcellation is derived from the full data sample ($n = 1{,}000$). Letters are displayed to aid visualization of the representation ordering. F, foot; H, hand; T, tongue; P, purple network; G, green network; O, orange network; R, red network. The colored networks refer to the 7-network parcellation (Fig. 8), and the somatomotor topography refers to the ordering as estimated in Fig. 5. G* refers to the minimal green network in the $x = -24$ section, which is better illustrated in Fig. 8 ($x = -8$). G− is highlighted because it does not follow the expected topographic pattern but rather may be an erroneous mapping, because it is located on the border between the cerebellum and cerebral cortex within a region of uncertain mapping (see Fig. 10). The white lines demarcate estimated boundaries between the maps and do not have significance in relation to sulcal boundaries. Three distinct representations are observed, labeled the primary, secondary, and tertiary representations. Each is a mirror-image ordering of the adjacent map. The question mark in the tertiary representation indicates the uncertain beginning point, if it does exist, of a third somatomotor representation. R* refers to the red network, which can be seen in the $x = -12$ section but not the $x = -24$ section. What appears initially as a complex pattern may be parsimoniously explained by the hypothesis that the major portion of the cerebellum contains a double, inverted representation of the entire cerebral cortex and then a potential tertiary representation in its most posterior extent. The classic observation of primary and secondary somatomotor representation in the anterior and posterior lobes may be the beginning and end points of much larger maps.

progression from somatomotor cortex to premotor cortex to association cortex. On the basis of quantitative analysis presented in Fig. 11, we can further hypothesize that the topographic mapping between the cerebrum and cerebellum is roughly homotopic, with the few exceptions discussed earlier and also the meager representation of the green network in the anterior lobe. Within this hypothesis, the established somatomotor maps are the end points of a much larger representation of the entire cerebral cortex.

There is also tentative evidence for a third map, as illustrated in Fig. 16. The tertiary map is mirrored relative to the adjacent secondary map, meaning its topography is inverted like that of the primary map beginning in the anterior lobe. We are not as confident about this tertiary map, because clear evidence for a tertiary somatomotor representation could not be detected (noted by the question mark in Fig. 16). However, the possibility of a tertiary representation may help to explain the robust representation of association cortex near lobule IX (e.g., Fig. 8, $x = -8$), in particular, association cortex coupled to the default network (Habas et al. 2009; Krienen and Buckner 2009). The large association region of the cerebellum near Crus I and II may represent the intersection of the primary and secondary maps; the cerebellar region near lobule IX may represent the association portion of the tertiary map. The hypothesized tertiary map may also explain a critical detail of prior anatomical work. In addition to extensive labeling of Crus II, Kelly and Strick (2003) also noted a small group of labeled neurons in IX/X in the monkey following anterograde transneuronal tracing of efferents from prefrontal area 46. This distinct region of labeled neurons is predicted by the hypothesis that the cerebellum possesses three topographic maps of the cerebral cortex. The neurons labeled in IX/X fall within the tertiary map.

Caveats and Limitations

In considering the possibility that the cerebellum has multiple, complete maps of the cerebral cortex, we must discuss several caveats and limitations. In particular, functional connectivity measures do not only reflect direct anatomy (Fox and Raichle 2007; Moeller et al. 2009; Buckner et al. 2010; Cole et al. 2010). Functional connectivity is based on correlated functional signals and thus cannot disambiguate whether a correlation reflects a direct coupling or an indirect effect of coupling among polysynaptically connected regions. This creates a specific ambiguity when proposing that the cerebellum has multiple maps of the cerebral cortex. A plausible alternative explanation is that one of the cerebellar maps represents coupling with frontal cortex and the other with parietal cortex, or some other combination of distributed cerebral areas. This ambiguity arises because each cerebral network has strongly coupled regions in both frontal and parietal cortices, including the somatomotor networks that span precentral (motor) and postcentral (somatosensory) gyrus. The functional connectivity data thus do not disambiguate whether the separate cerebellar maps arise from distinct cerebral areas or whether each map is interconnected with a distributed cerebral network. Further adding to this uncertainty, functional connectivity measures

also presently cannot disambiguate efferents from afferents.[2]

The transneuronal tracing data provide some insight. Injections of anterograde viral tracers in monkey M1 label distinct regions in the anterior and posterior lobes, suggesting that the individual frontal areas possess efferents to both the primary and secondary somatomotor representations within the cerebellum (see Fig. 8 of Kelly and Strick 2003). Similarly, area 46 efferents demonstrate dense labeling in Crus II and also a distinct second region in lobule IX/X. The presence of multiple cerebellar targets for each cerebral area is consistent with the possibility that multiple cerebellar maps form circuits with the same cerebral areas.

It will be important to assess in the future whether distributed cerebral areas converge on the same cerebellar regions. For example, parietal association cortex near 7a/opt is expected to project to the same cerebellar region as the prefrontal areas linked to the default network. Convergence of this form is seen for the thalamus. Double-labeling techniques reveal that multiple distributed cortical association areas—that are interconnected with each other—also receive convergent projections from the medial pulvinar (Goldman-Rakic 1988). We suspect that the cerebellum will possess a similar form of orderly topography.

The question of whether distributed cerebral areas within the same network converge on the same cerebellar regions is particularly critical, because the functional connectivity results do not directly tell us that prefrontal areas project to the cerebellum. The present results demonstrate that correlated networks of prefrontal and parietal association regions are coupled to the cerebellum. It seems unlikely, but remains a possibility, that the coupling is entirely driven by the parietal or other nonfrontal association areas. That is, the strong prefrontal coupling may be fully mediated through indirect correlations with posterior cerebral areas. The transneuronal tracing findings of Strick and colleagues (Middleton and Strick 1994, 2001; Kelly and Strick 2003) and the anterograde tracing studies of Schmahmann and Pandya (1997b), discussed earlier, suggest the presence of anatomical connections with prefrontal cortex. Nonetheless, anatomical studies of the distributed cerebral networks are required to determine which association areas directly form circuits with the cerebellum and which components of cerebral networks only interact indirectly with the cerebellum. Certain prefrontal regions that have shown lower densities of cerebellar projections (e.g., ventral area 46; Glickstein et al. 1985) may show functional coupling in our analyses via polysynaptic corticocortical connections.

A further open issue arises because we detected minimal evidence for medial to lateral organization within the cerebellum, as might be expected given the extensive evidence for longitudinal zones (see Ito 1984 for review). In this regard, it is important to note that the present work is cortical centric. The cerebellar cortex, particularly the intermediate zone, is the target of substantial ascending pathways that originate in the spinal cord. Our analyses did not explore these pathways, and important features of cerebellar organization may have been missed. The topographic maps estimated at present may also be of low resolution relative to other features of cerebellar organization such as those suggested by the observation of fractured somatotopy (Shambes et al. 1978; Manni and Petrosini 2004) and examination of topography in relation to the deep cerebellar nuclei. Similarly, assuming that some level of interdigitation of cerebral projection regions exists in the cerebellum, as in the striatum (Eblen and Graybiel 1995; Selemon and Goldman-Rakic 1985), our methods will obscure these details of the topography and assign the cerebellar regions to their most dominant principal cerebral targets. The specificity of the results in Figs. 13 and 15 suggests that the topography is unlikely to contain large amounts of overlap between distinct principal target regions. However, the low resolution of the technique may miss important features of cerebellar topography and the results should be interpreted accordingly.

Conclusions

Our results reveal that regions of the cerebellum are functionally coupled to specific cerebral networks. The results further suggest that a relatively simple principle might explain the global topographic organization of the cerebellum. The complete cerebral cortex (including somatomotor, premotor, and association cortices) may project to a homotopic map in the cerebellum that begins in the anterior lobe somatomotor representation and ends near Crus I/II. A mirror-image secondary map may then begin in Crus I/II and end with the second somatomotor representation near HVIII. Provisional evidence is also provided for a tertiary map at the farthest extent of the posterior lobe.

ACKNOWLEDGMENTS

We thank Jeremy Schmahmann for discussion, the Harvard Center for Brain Science Neuroimaging Core and the Athinoula A. Martinos Center for imaging support, the Harvard FAS Research Computing Group (in particular James Cuff, Jerry Lotto, and Jeff Chang), and the Neuroinformatics Research Group (Gabriele Fariello, Timothy O'Keefe, and Victor Petrov). We thank Haderer & Müller Biomedical Art for assistance with Fig. 5. F. M. Krienen was supported by fellowships from the Department of Defense, an Ashford Graduate Fellowship in the Sciences, and the Sackler Scholars Program in Psychobiology. A. Castellanos and J. C. Diaz were supported by the Howard Hughes Medical Institute Exceptional Research Opportunities Program.

GRANTS

This work was supported by National Institutes of Health Grants AG021910, P41 RR14074, and K08 MH067966, the Massachusetts General Hospital-University of California, Los Angeles Human Connectome Project (U54MH091665), the Howard Hughes Medical Institute, and the Simons Foundation.

DISCLAIMER

The content is solely the responsibility of the authors and does not necessarily represent the official views of the National Institutes of Health (NIH).

[2] As far as we have been able to surmise to date, the intrinsic functional correlations between the cerebellum and cerebral cortex are symmetrical. We have been unable to distinguish the cortico-pontocerebellar pathway from the cerebello-thalamocortical pathway. Focal pontine lesions disrupt fcMRI coupling between the cerebrum and cerebellum (Lu et al. in press). However, preliminary evidence also suggests that thalamic lesions do, as well (Lu J, Liu H, Buckner RL, and Li K, unpublished observations). Intrinsic fluctuations in the cerebellum may be coupled to intrinsic fluctuations in the cerebral cortex via an emergent property of the closed-loop circuit that involves both excitatory and inhibitory influences between the structures. Within this possibility, the correlated activity fluctuations between the structures should not be interpreted to differentially reflect the efferent or afferent projections, but rather the fluctuating activity of the full circuit.

DISCLOSURES

No conflicts of interest, financial or otherwise, are declared by the author(s).

REFERENCES

Adrian ED. Afferent areas in the cerebellum connected with the limbs. *Brain* 66: 289–315, 1943.

Allen G, McColl R, Barnard H, Ringe WK, Fleckenstein J, Cullum CM. Magnetic resonance imaging of the cerebellar-prefrontal and cerebellar-parietal functional connectivity. *Neuroimage* 28: 39–48, 2005.

Amunts K, Malikovic A, Mohlberg H, Schormann T, Zilles K. Brodmann's areas 17 and 18 brought into stereotaxic space—where and how variable? *Neuroimage* 11: 66–84, 2000.

Andrews-Hanna JR, Reidler JS, Sepulcre J, Poulin R, Buckner RL. Functional-anatomic fractionation of the brain's default network. *Neuron* 65: 550–562, 2010.

Balsters JH, Cussans E, Diedrichsen J, Phillips KA, Preuss TM, Rilling JK, Ramnani N. Evolution of the cerebellar cortex: the selective expansion of prefrontal-projecting cerebellar lobules. *Neuroimage* 49: 2045–2052, 2010.

Ben-Yehudah G, Guediche S, Fiez JA. Cerebellar contributions to verbal working memory: beyond cognitive theory. *Cerebellum* 6: 193–201, 2007.

Birn RM, Diamond JB, Smith MA, Bandettini PA. Separating respiratory-variation-related fluctuations from neuronal-activity-related fluctuations in fMRI. *Neuroimage* 31: 1536–1548, 2006.

Biswal B, Yetkin FZ, Haughton VM, Hyde JS. Functional connectivity in the motor cortex of resting human brain using echo-planar MRI. *Magn Reson Med* 34: 537–541, 1995.

Biswal BB, Mennes M, Zuo XN, Gohel S, Kelly C, Smith SM, Beckmann CF, Adelstein JS, Buckner RL, Colcombe S, Dogonowski AM, Ernst M, Fair D, Hampson M, Hoptman MJ, Hyde JS, Kiviniemi VJ, Kotter R, Li SJ, Lin CP, Lowe MJ, Mackay C, Madden DJ, Madsen KH, Margulies DS, Mayberg HS, McMahon K, Monk CS, Mostofsky SH, Nagel BJ, Pekar JJ, Peltier SJ, Petersen SE, Riedl V, Rombouts SARB, Rypma B, Schlaggar BL, Schmidt S, Seidler RD, Siegle GJ, Sorg C, Teng GJ, Veijola J, Villringer A, Walter M, Wang L, Weng XC, Whitfield-Gabrieli S, Williamson P, Windischberger C, Zang YF, Zhang HY, Castellanos FX, Milham MP. Toward discovery science of human brain function. *Proc Natl Acad Sci USA* 107: 4734–4739, 2010.

Brodal P. The corticopontine projection in rhesus-monkey: origin and principles of organization. *Brain* 101: 251–283, 1978.

Buckner RL. Human functional connectivity: new tools, unresolved questions. *Proc Natl Acad Sci USA* 107: 10769–10770, 2010.

Buckner RL, Andrews-Hanna JR, Schacter DL. The brain's default network: anatomy, function, and relevance to disease. *Ann NY Acad Sci* 1124: 1–38, 2008.

Cole DM, Smith SM, Beckmann CF. Advances and pitfalls in the analysis and interpretation of resting-state FMRI data. *Front Syst Neurosci* 4: 8, 2010.

Cowey A. Projection of retina on to striate and prestriate cortex in squirrel monkey, *Saimiri sciureus*. *J Neurophysiol* 27: 366–393, 1964.

Dale AM, Fischl B, Sereno MI. Cortical surface-based analysis. I. Segmentation and surface reconstruction. *Neuroimage* 9: 179–194, 1999.

Desmond JE, Fiez JA. Neuroimaging studies of the cerebellum: language, learning and memory. *Trends Cogn Sci* 2: 355–362, 1998.

Di Martino A, Scheres A, Margulies DS, Kelly AMC, Uddin LQ, Shehzad Z, Biswal B, Walters JR, Castellanos FX, Milham MP. Functional connectivity of human striatum: a resting state fMRI study. *Cereb Cortex* 18: 2735–2747, 2008.

Dickson J, Drury H, Van Essen DC. 'The surface management system' (SuMS) database: a surface-based database to aid cortical surface reconstruction, visualization and analysis. *Philos Trans R Soc Lond B Biol Sci* 356: 1277–1292, 2001.

Diedrichsen J, Balsters JH, Flavell J, Cussans E, Ramnani N. A probabilistic MR atlas of the human cerebellum. *Neuroimage* 46: 39–46, 2009.

Dosenbach NUF, Fair DA, Miezin FM, Cohen AL, Wenger KK, Dosenbach RAT, Fox MD, Snyder AZ, Vincent JL, Raichle ME, Schlaggar BL, Petersen SE. Distinct brain networks for adaptive and stable task control in humans. *Proc Natl Acad Sci USA* 104: 11073–11078, 2007.

Durisko C, Fiez JA. Functional activation in the cerebellum during working memory and simple speech tasks. *Cortex* 46: 896–906, 2010.

Eblen F, Graybiel AM. Highly restricted origin of prefrontal cortical inputs to striosomes in the macaque monkey. *J Neurosci* 15: 5999–6013, 1995.

Evans AC, Collins DL, Mills SR, Brown ED, Kelly RL, Peters TM. 3D statistical neuroanatomical models from 305 MRI volumes. *Proceedings IEEE Nuclear Science Symposium and Medical Imaging Conference*. London: MTP, 1993, vol. 95, p. 1813–1817.

Evarts EV, Thach WT. Motor mechanisms of the CNS: cerebrocerebellar interrelations. *Annu Rev Physiol* 31: 451–498, 1969.

Fischl B, Liu A, Dale AM. Automated manifold surgery: constructing geometrically accurate and topologically correct models of the human cerebral cortex. *IEEE Trans Med Imaging* 20: 70–80, 2001.

Fischl B, Rajendran N, Busa E, Augustinack J, Hinds O, Yeo BTT, Mohlberg H, Amunts K, Zilles K. Cortical folding patterns and predicting cytoarchitecture. *Cereb Cortex* 18: 1973–1980, 2008.

Fischl B, Salat DH, Busa E, Albert M, Dieterich M, Haselgrove C, van der Kouwe A, Killiany R, Kennedy D, Klaveness S, Montillo A, Makris N, Rosen B, Dale AM. Whole brain segmentation: automated labeling of neuroanatomical structures in the human brain. *Neuron* 33: 341–355, 2002.

Fischl B, Salat DH, van der Kouwe AJW, Makris N, Ségonne F, Quinn BT, Dale AM. Sequence-independent segmentation of magnetic resonance images. *Neuroimage* 23: S69–S84, 2004.

Fischl B, Sereno MI, Dale AM. Cortical surface-based analysis. II: Inflation, flattening, and a surface-based coordinate system. *Neuroimage* 9: 195–207, 1999a.

Fischl B, Sereno MI, Tootell RBH, Dale AM. High-resolution intersubject averaging and a coordinate system for the cortical surface. *Hum Brain Mapp* 8: 272–284, 1999b.

Fonov V, Evans AC, Botteron K, Almli CR, McKinstry RC, Collins DL, Brain Development Cooperative Group. Unbiased average age-appropriate atlases for pediatric studies. *Neuroimage* 54: 313–327, 2011.

Fox MD, Raichle ME. Spontaneous fluctuations in brain activity observed with functional magnetic resonance imaging. *Nat Rev Neurosci* 8: 700–711, 2007.

Fox MD, Zhang DY, Snyder AZ, Raichle ME. The global signal and observed anticorrelated resting state brain networks. *J Neurophysiol* 101: 3270–3283, 2009.

Friston KJ, Ashburner J, Frith CD, Poline JB, Heather JD, Frackowiak RSJ. Spatial registration and normalization of images. *Hum Brain Mapp* 3: 165–189, 1995.

Geyer S, Ledberg A, Schleicher A, Kinomura S, Schormann T, Bürgel U, Klingberg T, Larsson J, Zilles K, Roland PE. Two different areas within the primary motor cortex of man. *Nature* 382: 805–807, 1996.

Glickstein M, May JG, Mercier BE. Corticopontine projection in the macaque: the distribution of labeled cortical cells after large injections of horseradish-peroxidase in the pontine nuclei. *J Comp Neurol* 235: 343–359, 1985.

Glickstein M. What does the cerebellum really do? *Curr Biol* 17: R824–R827, 2007.

Goldman-Rakic PS. Topography of cognition: parallel distributed networks in primate association cortex. *Annu Rev Neurosci* 11: 137–156, 1988.

Grefkes C, Geyer S, Schormann T, Roland P, Zilles K. Human somatosensory area 2: observer-independent cytoarchitectonic mapping, interindividual variability and population map. *Neuroimage* 14: 617–631, 2001.

Greve DN, Fischl B. Accurate and robust brain image alignment using boundary-based registration. *Neuroimage* 48: 63–72, 2009.

Grodd W, Hulsmann E, Lotze M, Wildgruber D, Erb M. Sensorimotor mapping of the human cerebellum: fMRI evidence of somatotopic organization. *Hum Brain Mapp* 13: 55–73, 2001.

Habas C, Kamdar N, Nguyen D, Prater K, Beckmann CF, Menon V, Greicius MD. Distinct cerebellar contributions to intrinsic connectivity networks. *J Neurosci* 29: 8586–8594, 2009.

Hill J, Inder T, Neil J, Dierker D, Harwell J, Van Essen D. Similar patterns of cortical expansion during human development and evolution. *Proc Natl Acad Sci USA* 107: 13135–13140, 2010.

Holmes G. The cerebellum of man. *Brain* 62: 1–30, 1939.

Ito M. *The Cerebellum and Neural Control*. New York: Raven, 1984.

Jenkinson M, Bannister P, Brady M, Smith S. Improved optimization for the robust and accurate linear registration and motion correction of brain images. *Neuroimage* 17: 825–841, 2002.

Kahn I, Andrews-Hanna JR, Vincent JL, Snyder AZ, Buckner RL. Distinct cortical anatomy linked to subregions of the medial temporal lobe revealed by intrinsic functional connectivity. *J Neurophysiol* 100: 129–139, 2008.

Kelly RM, Strick PL. Cerebellar loops with motor cortex and prefrontal cortex of a nonhuman primate. *J Neurosci* 23: 8432–8444, 2003.

Kemp JM, Powell TPS. The connexions of the striatum and globus pallidus: synthesis and speculation. *Philos Trans R Soc Lond B Biol Sci* 262: 441–457, 1971.

Krienen FM, Buckner RL. Segregated fronto-cerebellar circuits revealed by intrinsic functional connectivity. *Cereb Cortex* 19: 2485–2497, 2009.

Kwong KK, Belliveau JW, Chesler DA, Goldberg IE, Weisskoff RM, Poncelet BP, Kennedy DN, Hoppel BE, Cohen MS, Turner R, Cheng HM, Brady TJ, Rosen BR. Dynamic magnetic resonance imaging of human brain activity during primary sensory stimulation. *Proc Natl Acad Sci USA* 89: 5675–5679, 1992.

Laird AR, Fox PM, Price CJ, Glahn DC, Uecker AM, Lancaster JL, Turkeltaub PE, Kochunov P, Fox PT. ALE meta-analysis: controlling the false discovery rate and performing statistical contrasts. *Hum Brain Mapp* 25: 155–64, 2005.

Larsell O. *The Comparative Anatomy and Histology of the Cerebellum From Monotremes Through Apes.* Minneapolis, MN: The University of Minnesota Press, 1970.

Leiner HC, Leiner AL, Dow RS. Does the cerebellum contribute to mental skills? *Behav Neurosci* 100: 443–454, 1986.

Leiner HC. Solving the mystery of the human cerebellum. *Neuropsychol Rev* 20: 229–235, 2010.

Lu J, Liu H, Zhang M, Wang D, Cao Y, Ma Q, Rong D, Wang X, Buckner RL, Li K. Focal pontine lesions provide evidence that resting-state functional connectivity reflects polysynaptic anatomical pathways. *J Neurosci*. In press.

Malikovic A, Amunts K, Schleicher A, Mohlberg H, Eickhoff SB, Wilms M, Palomero-Gallagher N, Armstrong E, Zilles K. Cytoarchitectonic analysis of the human extrastriate cortex in the region of V5/MT+: a probabilistic, stereotaxic map of area hOc5. *Cereb Cortex* 17: 562–574, 2007.

Manni E, Petrosini L. A century of cerebellar somatotopy: a debated representation. *Nat Rev Neurosci* 5: 241–249, 2004.

Marcus DS, Fotenos AF, Csernansky JG, Morris JC, Buckner RL. Open access series of imaging studies: longitudinal MRI data in nondemented and demented older adults. *J Cogn Neurosci* 22: 2677–2684, 2010.

Marcus DS, Wang TH, Parker J, Csernansky JG, Morris JC, Buckner RL. Open access series of imaging studies (OASIS): cross-sectional MRI data in young, middle aged, nondemented, and demented older adults. *J Cogn Neurosci* 19: 1498–1507, 2007.

Margulies DS, Kelly AMC, Uddin LQ, Biswal BB, Castellanos FX, Milham MP. Mapping the functional connectivity of anterior cingulate cortex. *Neuroimage* 37: 579–588, 2007.

Marvel CL, Desmond JE. The contributions of cerebro-cerebellar circuitry to executive verbal working memory. *Cortex* 46: 880–895, 2010.

Middleton FA, Strick PL. Anatomical evidence for cerebellar and basal ganglia involvement in higher cognitive function. *Science* 266: 458–461, 1994.

Middleton FA, Strick PL. Cerebellar projections to the prefrontal cortex of the primate. *J Neurosci* 21: 700–712, 2001.

Moeller S, Nallasamy N, Tsao DY, Freiwald WA. Functional connectivity of the macaque brain across stimulus and arousal states. *J Neurosci* 29: 5897–5909, 2009.

Murphy K, Birn RM, Handwerker DA, Jones TB, Bandettini PA. The impact of global signal regression on resting state correlations: are anti-correlated networks introduced? *Neuroimage* 44: 893–905, 2009.

Ogawa S, Tank DW, Menon R, Ellermann JM, Kim SG, Merkle H, Ugurbil K. Instrinsic signal changes accompanying sensory stimulation: functional brain mapping with magnetic resonance imaging. *Proc Natl Acad Sci USA* 89: 5951–5955, 1992.

O'Reilly JX, Beckmann CF, Tomassini V, Ramnani N, Johansen-Berg H. Distinct and overlapping functional zones in the cerebellum defined by resting state functional connectivity. *Cereb Cortex* 20: 953–965, 2010.

O'Reilly JX, Mesulam MM, Nobre AC. The cerebellum predicts the timing of perceptual events. *J Neurosci* 28: 2252–2260, 2008.

Pandya DN, Vignolo LA. Intra- and interhemispheric projections of the precentral, premotor and arcuate areas in the rhesus monkey. *Brain Res* 26: 217–233, 1971.

Petersen SE, Fox PT, Posner MI, Mintun M, Raichle ME. Positron emission tomographic studies of the processing of single words. *J Cogn Neurosci* 1: 153–170, 1989.

Preuss TM. What is it like to be human? In: *The Cognitive Neurosciences III*, edited by Gazzaniga M. Cambridge, MA: MIT Press, 2004, p. 5–22.

Raichle ME, MacLeod AM, Snyder AZ, Powers WJ, Gusnard DA, Shulman GL. A default mode of brain function. *Proc Natl Acad Sci USA* 98: 676–682, 2001.

Raichle ME. The restless brain. *Brain Connect* 1: 3–12, 2011.

Roy AK, Shehzad Z, Margulies DS, Kelly AMC, Uddin LQ, Gotimer K, Biswal BB, Castellanos FX, Milham MP. Functional connectivity of the human amygdala using resting state fMRI. *Neuroimage* 45: 614–626, 2009.

Schlerf JE, Verstynen TD, Ivry RB, Spencer RMS. Evidence of a novel somatotopic map in the human neocerebellum during complex actions. *J Neurophysiol* 103: 3330–3336, 2010.

Schmahmann JD, Doyon J, McDonald D, Holmes C, Lavoie K, Hurwitz AS, Kabani N, Toga A, Evans AC, Petrides M. Three-dimensional MRI atlas of the human cerebellum in proportional stereotaxic space. *Neuroimage* 10: 233–260. 1999.

Schmahmann JD, Doyon J, Toga AW, Petrides M, Evans AC. *MRI Atlas of the Human Cerebellum.* San Diego, CA: Academic, 2000.

Schmahmann JD, Pandya DN. The cerebrocerebellar system. *Int Rev Neurobiol* 41: 31–60, 1997a.

Schmahmann JD, Pandya DN. Anatomic organization of the basilar pontine projections from prefrontal cortices in rhesus monkey. *J Neurosci* 17: 438–458, 1997b.

Schmahmann JD, Rosene DL, Pandya DN. Motor projections to the basis pontis in the rhesus monkey. *J Comp Neurol* 478: 248–268, 2004a.

Schmahmann JD, Rosene DL, Pandya DN. Ataxia after pontine stroke: insights from pontocerebellar fibers in monkey. *Ann Neurol* 55: 585–589, 2004b.

Schmahmann JD, Weilburg JB, Sherman JC. The neuropsychiatry of the cerebellum—insights from the clinic. *Cerebellum* 6: 254–267, 2007.

Seeley WW, Menon V, Schatzberg AF, Keller J, Glover GH, Kenna H, Reiss AL, Greicius MD. Dissociable intrinsic connectivity networks for salience processing and executive control. *J Neurosci* 27: 2349–2356, 2007.

Ségonne F, Dale AM, Busa E, Glessner M, Salat D, Hahn HK, Fischl B. A hybrid approach to the skull stripping problem in MRI. *Neuroimage* 22: 1060–1075, 2004.

Ségonne F, Pacheco J, Fischl B. Geometrically accurate topology-correction of cortical surfaces using nonseparating loops. *IEEE Trans Med Imaging* 26: 518–529, 2007.

Selemon LD, Goldman-Rakic PS. Longitudinal topography and interdigitation of corticostriatal projections in the rhesus monkey. *J Neurosci* 5: 776–794, 1985.

Shambes GM, Gibson JM, Welker W. Fractured somatotopy in granule cell tactile areas of rat cerebellar hemispheres revealed by micromapping. *Brain Behav Evol* 15: 94–140, 1978.

Smith SM, Jenkinson M, Woolrich MW, Beckmann CF, Behrens TEJ, Johansen-Berg H, Bannister PR, De Luca M, Drobnjak I, Flitney DE, Niazy RK, Saunders J, Vickers J, Zhang Y, De Stefano N, Brady JM, Matthews PM. Advances in functional and structural MR image analysis and implementation as FSL. *Neuroimage* 23: S208–S219, 2004.

Snider RS, Eldred E. Cerebro-cerebellar relationships in the monkey. *J Neurophysiol* 15: 27–40, 1952.

Snider RS, Stowell A. Receiving areas of the tactile, auditory and visual systems in the cerebellum. *J Neurophysiol* 7: 331–357, 1944.

Spencer RMC, Verstynen T, Brett M, Ivry R. Cerebellar activation during discrete and not continuous timed movements: an fMRI study. *Neuroimage* 36: 378–387, 2007.

Stoodley CJ, Schmahmann JD. Functional topography in the human cerebellum: a meta-analysis of neuroimaging studies. *Neuroimage* 44: 489–501, 2009.

Strick PL, Dum RP, Fiez JA. Cerebellum and nonmotor function. *Annu Rev Neurosci* 32: 413–434, 2009.

Strick PL. How do the basal ganglia and cerebellum gain access to the cortical motor areas? *Behav Brain Res* 18: 107–123, 1985.

Timmann D, Daum I. Cerebellar contributions to cognitive functions: a progress report after two decades of research. *Cerebellum* 6: 159–162, 2007.

van der Kouwe AJW, Benner T, Fischl B, Schmitt F, Salat DH, Harder M, Sorensen AG, Dale AM. On-line automatic slice positioning for brain MR imaging. *Neuroimage* 27: 222–230, 2005.

van der Kouwe AJW, Benner T, Salat DH, Fischl B. Brain morphometry with multiecho MPRAGE. *Neuroimage* 40: 559–569, 2008.

Van Dijk KRA, Hedden T, Venkataraman A, Evans KC, Lazar SW, Buckner RL. Intrinsic functional connectivity as a tool for human connectomics: theory, properties, and optimization. *J Neurophysiol* 103: 297–321, 2010.

Van Essen DC. A population-average, landmark-and surface-based (PALS) atlas of human cerebral cortex. *Neuroimage* 28: 635–662, 2005.

Van Essen DC. Surface-based atlases of cerebellar cortex in the human, macaque and mouse. *Ann NY Acad Sci* 978: 468–479, 2002.

Van Essen DC, Dierker DL. Surface-based and probabilistic atlases of primate cerebral cortex. *Neuron* 56: 209–225, 2007.

Van Essen DC, Newsome WT, Bixby JL. The pattern of interhemispheric connections and its relationship to extrastriate visual areas in the macaque monkey. *J Neurosci* 2: 265–283, 1982.

Vincent JL, Snyder AZ, Fox MD, Shannon BJ, Andrews JR, Raichle ME, Buckner RL. Coherent spontaneous activity identifies a hippocampal-parietal memory network. *J Neurophysiol* 96: 3517–3531, 2006.

Wandell BA, Dumoulin SO, Brewer AA. Visual field maps in human cortex. *Neuron* 56: 366–383, 2007.

Wiestler T, McGonigle DJ, Diedrichsen J. Integration of sensory and motor representations of single fingers in the human cerebellum. *J Neurophysiol* 105: 3042–3053, 2011.

Wilms M, Eickhoff SB, Specht K, Amunts K, Shah NJ, Malikovic A, Fink GR. Human V5/MT+: comparison of functional and cytoarchitectonic data. *Anat Embryol* 210: 485–495, 2005.

Wise RG, Ide K, Poulin MJ, Tracey I. Resting fluctuations in arterial carbon dioxide induce significant low frequency variations in BOLD signal. *Neuroimage* 21: 1652–1664, 2004.

Yeo BTT, Krienen FM, Sepulcre J, Sabuncu MR, Lashkari L, Hollinshead M, Roffman JL, Smoller JW, Zöllei L, Polimeni JR, Fischl B, Liu H, Buckner RL. The organization of the human cerebral cortex estimated by intrinsic functional connectivity. *J Neurophysiol* 106: 1125–1165, 2011.

Yeo BTT, Sabuncu MR, Vercauteren T, Holt DJ, Amunts K, Zilles K, Golland P, Fischl B. Learning task-optimal registration cost functions for localizing cytoarchitecture and function in the cerebral cortex. *IEEE Trans Med Imaging* 29: 1424–1441, 2010.

Zhang D, Snyder AZ, Fox MD, Sansbury MW, Shimony JS, Raichle ME. Intrinsic functional relations between human cerebral cortex and thalamus. *J Neurophysiol* 100: 1740–1748, 2008.